

EFFICIENCY OPTIMIZATION OF INDUCTION MOTOR DRIVE USING LOSS MODEL CONTROL

A DISSERTATION

*Submitted in partial fulfillment of the
requirements for the award of the degree*

of

INTEGRATED DUAL DEGREE

(Bachelor of Technology & Master of Technology)

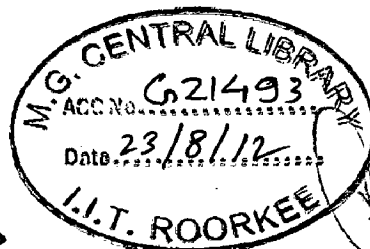
in

ELECTRICAL ENGINEERING

(With Specialization in Power Electronics)

By

ANIL CHANDRAKANTH.S



**DEPARTMENT OF ELECTRICAL ENGINEERING
INDIAN INSTITUTE OF TECHNOLOGY ROORKEE
ROORKEE - 247 667 (INDIA)
JUNE, 2012**

I.D.NO. MT/192/SPS/55

CANDIDATES DECLARATION

I hereby certify that the dissertation titled "EFFICIENCY OPTIMIZATION OF INDUCTION MOTOR DRIVE USING LOSS MODEL CONTROL" being submitted by me in partial fulfillment of the requirement for the award of degree of Integrated Dual Degree in Electrical Engineering with specialization in "Power Electronics" at I.I.T. Roorkee is a bonafide work carried by me under the supervision of Prof.S.P.Srivastava in Electrical Engineering, I.I.T. Roorkee. I have not submitted the matter embodied in this dissertation report in any other University for the award of any other degree.


Date: 15-06-2012

Place: Roorkee


ANIL CHANDRAKANTH.S
IDD 5th Year

Department of Electrical Engineering
I.I.T. Roorkee

This is to certify that the above declaration made by candidate is correct to the best of my knowledge.


Dr.S.P.SRIVASTAVA
Professor
Department of Electrical Engineering
I.I.T.Roorkee
Roorkee-247667

ACKNOWLEDGEMENT

I would like to express my deep sense of gratitude and sincere thanks to **Dr. S.P. Srivastava**, Professor, Department of Electrical Engineering, Indian Institute of Technology, for his esteem guidance, valuable suggestions and caring nature without which it would not have been possible to compile this dissertation report in present form.

I thank **Mr. C. Thanga Raj**, Asst. Professor, WRDM Department, for his valuable suggestions and support.

I am extremely grateful to my parents, friends and well-wishers for their candid help, meaningful suggestions and persistent encouragement given to me at different stages of my work.

Date: 15-06-2012
Place: Roorkee

ANIL CHANDRAKANTH.S
Enrolment.no-071601

ABSTRACT

Due to robustness, reliability, low price and maintenance free, induction motors (IMs) are used in most of the industrial applications. The influence of these motors (in terms of energy consumption) in energy intensive industries is significant in total input cost. Optimal control covers both the broad approaches namely, loss model control (LMC) and search control (SC). This report primarily focuses on efficiency optimisation of induction motor drive through loss model control.

Induction motor is a high efficiency electrical machine when working close to its rated torque and speed. However, at light loads, no balance in between copper and iron losses, results considerable reduction in the efficiency. The part load efficiency and power factor can be improved by making the motor excitation adjustment in accordance with load and speed. To implement the above goal, the induction motor should either be fed through an inverter or redesigned with optimization algorithms.

For optimal energy control of induction motor, flux level in a machine is adjusted to give minimum operating cost for the industrial load. The flux controller improves the economics in terms of operating cost and test results show that the flux level in the most economic motor is adjusted according to load and speed, particular at light load.

In the present work, induction motor loss model is developed and optimal value of flux is obtained through the motor loss model to give maximum efficiency of the motor. Maximum and minimum levels of flux and stator currents are forced as constraints in the algorithm. Here, loss model controller is designed and implemented for different variations in speed and torque. DC-link power is measured in each case and is compared with that of conventional constant flux control technique. Mine hoist diagram used in mineral industry is also considered as a practical example and the effect of LMC on it is studied. Induction motor parameters vary with temperature. So, parameters obtained by conducting no load and blocked rotor test may vary with loading of induction motor. LMC is sensitive to parameter variation and its performance is affected when parameters change. An attempt is made to gain a deeper physical insight into the induction motor operation through sensitivity analysis of LMC under parameter variation. The study reveals the effect each of the circuit parameters namely R_s , R_r , L_s , L_r and L_m has on torque, speed, flux and DC-link power respectively.

Table of Contents

CONTENTS

TITLE	PAGE NO.
Candidates declaration	i
Acknowledgements	ii
Abstract	iii
Table of Contents	iv
List of Figures	viii
List of Tables	x
List of symbols	xi
Chapter1: Introduction	1
1.1 Introduction	1
1.2 Statement of problem	2
1.3 Literature review	2
1.4 Organization of dissertation	4
Chapter2: 3- Φ Induction Motor and Different types of Losses in Induction Motor	5
2.1 Introduction	5

2.2 Losses in Induction Motor	6
2.2.1 Copper losses	6
2.2.1.1 Stator copper losses	6
2.2.1.2 Rotor copper losses	7
2.2.2 Core losses	7
2.2.3 Stray load loss	9
2.2.4 Mechanical losses	10
2.3 Efficiency maximization	11
2.4 Conclusion	12
Chapter 3. Optimal Controllers for Induction Motor Drive	13
3.1 Introduction	13
3.2 Loss model controller (LMC)	14
3.2.1 Scalar Controlled Drives	15
3.2.2 Vector Controlled Drives	16
3.3 Search Controller	17
3.3.1 Scalar Controlled Drives	18
3.3.2 Vector controlled Drives	18
3.3.3 AI and NIA Based Controllers	18
3.3.4 Both LMC and Search Control	19
3.4 Loss Model Controller vs. Search Controller:	19

3.5 Conclusion	20
Chapter4: Modeling of Energy Efficient Controllers	21
4.1 Introduction:	21
4.2 Modelling of LMC	21
4.3 Modelling of search controller	26
4.4 Conclusion	28
Chapter5: In-situ Efficiency Determination of Induction Motor through Parameter Estimation	29
5.1 Introduction	29
5.2 Standards for induction motor efficiency determination	31
5.2.1 IEEE method 112-1996	31
5.2.2 IEC 34-2 method	32
5.2.3 JEC method	32
5.3 Optimization algorithm used	33
5.4 In-situ Efficiency determination:	33
5.5 Experimental setup and parameter settings	37
5.5.1 Experimental setup	37
5.5.2 Parameter settings	38
5.6 Results and Discussion	40

5.7 Conclusion	40
Chapter6: Simulation Results and Discussions	41
6.1 Introduction	41
6.2 Results	42
Chapter7: Conclusion	63
7.1 Conclusion	63
7.2 Future scope	64
References	65
List of Publications	68
Appendix-A	69

List of figures

Fig. 3.1	Scalar controlled drive using LMC	16
Fig. 3.2	Vector controlled drive using LMC	17
Fig. 4.1	Space vector equivalent circuit in a rotor-flux-oriented reference frame including an iron loss resistor	21
Fig. 4.2	Phasor diagram of equivalent circuits and rotor field angle definition	22
Fig. 4.3	Steady state equivalent circuit of IM on d, q axes respectively	23
Fig. 4.4	Overall block diagram of proposed loss model based induction motor drive	26
Fig. 4.5	Ramp search method	27
Fig. 4.6	Flow chart of Search controller	28
Fig. 5.1	Block diagram of induction motor in-situ efficiency determination	34
Fig. 5.2	Winding arrangement of star connected motor	34
Fig. 5.3	Equivalent circuit of induction motor with stray loss resistance	35
Fig. 5.4	Experimental setup for determining induction motor efficiency	37
Fig. 5.5	Comparison of measured and estimated (i) line currents and (ii) power factor of 3.74 KW induction motor respectively	39
Fig. 5.6	Comparison of error in efficiency for different standards and at different load points for objective function (i) ff_1 and (ii) ff_2	40
Fig. 6.1	Load diagram when only load is changed	42
Fig. 6.2	Simulation results of vector controlled induction motor drive without loss model control (load changes)	44
Fig. 6.3	Simulation results of vector controlled induction motor drive with loss model control (load changes)	46
Fig. 6.4	Load diagram when only speed is changed	47
Fig. 6.5	Simulation results of vector controlled induction motor drive without loss model control (speed changes)	49
Fig. 6.6	Simulation results of energy efficient vector controlled induction motor drive with loss model control (speed changes)	51
Fig. 6.7	Mine hoist load diagram	52

Fig. 6.8	Simulation results of vector controlled induction motor drive without loss model control (load, speed change)	54
Fig. 6.9	Simulation results of energy efficient vector controlled induction motor drive with loss model control (load, speed change)	56
Fig.6.10	Load diagram for sensitivity analysis of LMC under parameter variation	57
Fig.6.11	Simulation results of vector controlled induction motor drive with LMC under normal operating conditions when none of the parameters is varied ($R_s = 11.124$ ohm; $R_r = 8.9838$ ohm; $L_s = 33.36$ mH; $L_m = 0.49045$ mH; $L_r = 33.36$ mH)	58
Fig.6.12	Simulation results of vector controlled induction motor drive with LMC when R_s is increased by 20% ($R_s = 13.3488$ ohm; $R_r = 8.9838$ ohm; $L_s = 33.36$ mH, $L_m = 490.45$ mH, $L_r = 33.36$ mH)	58
Fig.6.13	Simulation results of vector controlled induction motor drive with LMC when R_r is increased by 20% ($R_s = 11.124$ ohm; $R_r = 10.78056$ ohm; $L_s = 33.36$ mH; $L_m = 490.45$ mH, $L_r = 33.36$ mH)	58
Fig.6.14	Simulation results of vector controlled induction motor drive with LMC when L_s is increased by 20% ($R_s = 11.124$ ohm; $R_r = 8.9838$ ohm; $L_s = 40.032$ mH; $L_m = 490.45$ mH; $L_r = 33.36$ mH)	59
Fig.6.15	Simulation results of vector controlled induction motor drive with LMC when L_r is increased by 20% ($R_s = 11.124$ ohm; $R_r = 8.9838$ ohm; $L_s = 33.36$ mH; $L_m = 490.45$ mH; $L_r = 33.36$ mH)	59
Fig.6.16	Simulation results of vector controlled induction motor drive with LMC when L_m is decreased by 20% ($R_s = 11.124$ ohm; $R_r = 8.9838$ ohm; $L_s = 33.36$ mH; $L_m = 392.36$ mH; $L_r = 33.36$ mH)	59
Fig. A.1	MATLAB/SIMULINK model of loss model control of induction motor	67
Fig. A.2	Discrete PI controller in MATLAB	68
Fig. A.3	Vector controller	69
Fig. A.4	MATLAB model for the estimation of i_{ds}^* , i_{qs}^* and ω_2^* .	70
Fig. A.5	MATLAB model for calculating flux angle	71
Fig. A.6	MATLAB model for finding out three phase reference currents	71

List of tables

Table 5.1	Stray Load Losses for the Different Capacity Motors (IEEE standard 2004)	35
Table 5.2	Voltage, current, power input, speed and power factor at various load points	38
Table 5.3	Efficiency calculation of induction motor by IEEE	38
Table 5.4	Efficiency calculation of induction motor by IEC	38
Table 5.5	Efficiency calculation of induction motor by JEC	39
Table 5.6	Error calculation for different standards using objective functions ff_1 , ff_2	39
Table 6.1	Induction Motor Parameters for Simulation	41
Table 6.2	Motor performance when parameters are changed by 20% under LMC operation	60
Table 6.3	Motor performance when parameters are changed by 20% under constant flux operation	60
Table 6.4	Motor performance when parameters are changed by 10% under LMC operation	61
Table 6.5	Motor performance when parameters are changed by 10% under constant flux operation	61

List of symbols

R_s, R_r	resistances of a stator and rotor phase winding
L_s, L_r	self inductance of the stator and the rotor
L_m	magnetizing inductance
σ	leakage factor ($1 - L_m^2 / (L_s L_r)$)
R_r'	referred rotor resistance $R_r' = (L_m / L_r)^2 R_r$
L_s'	referred stator inductance ($L_s' = \sigma L_s$)
L_m'	referred magnetizing inductance ($L_m' = (1 - \sigma) L_s$)
Z_p	number of pole pairs
ω_e	angular speed of the rotor flux ($\omega_e = d\theta_e/dt$)
ω_r	electrical rotor speed ($\omega_r = d\theta_r/dt$)
ω_m	mechanical rotor speed ($\omega_m = d\theta_m/dt$)
ω_{ref}	mechanical rotor reference speed
i_{mR}	rotor magnetizing current
u_s, i_s	stator voltage and current complex space vector
I_{ds}	d-axis stator current
I_{qs}	q-axis stator current
Φ_m	mutual flux or air-gap flux
K_h	hysteresis loss coefficient
K_e	eddy current loss coefficient
K_c	flux constant
P_e	eddy current power loss
P_h	hysteresis power loss
ω_r	speed of the rotor
ω_e	synchronous speed of the stator
C_{fw}	mechanical power loss coefficient
T_e	electro magnetic torque
T_l	load torque
J	inertia of rotor
Θ_e	stator flux angle

Θ_r	rotor flux angle
R_q	q-axis equivalent resistance
R_d	d axis equivalent resistance
K_t	torque constant
K	loss factor

Introduction

[This chapter consists of the introduction of work done in thesis. It gives the statement of the problem and review of the previous stepwise growth of the work done in this field. The organization of dissertation is given in the end of the chapter.]

1.1 Introduction:

More than 50% of the electrical energy produced is consumed by motors and induction motors are one of the most widely used motors in electrical drives because of their reliability, ruggedness and relatively low cost [1]. Electrical motor drive losses consist of grid loss, converter loss, motor loss and transmission loss. In an effort to improve efficiency, there have been improvements in the materials, design and construction techniques. However, converter loss and motor loss are still greatly dependent on control strategies, especially when the motor operates at light load. Induction motor is a high efficiency electrical machine when working close to its rated torque and speed. However, at light loads, no balance in between copper and iron losses, results considerable reduction in the efficiency. The part load efficiency and power factor can be improved by making the motor excitation adjustment in accordance with load and speed. To implement the above goal, the induction motor should either be fed through an inverter or redesigned with optimization algorithm.

The control strategy to improve motor efficiency can be divided into two categories [1]:

- 1) Search controller (SC)
- 2) Loss model controller (LMC)

1.1.1 Search controller (SC):

Basic principle: It measures the input power and then iteratively searches for the flux level (or its equivalent variables) until the minimum input power is detected for a given torque and speed [2].

Drawbacks: Slow convergence and torque ripples [1].

1.1.2 Loss-model-based controller (LMC):

Basic principle: The loss model controller computes losses by using the machine model and selects a flux level that minimizes the losses [1]. LMC is fast and does not produce torque ripples. However, the accuracy depends on the correct modelling of the motor drive and the losses.

1.2 Statement of problem:

The main aim of the dissertation is to design Loss Model controller, which can increase the efficiency of the induction motor under light load conditions. This work is not a one step work but includes a lot of small jobs in it. The breakup of the dissertation work done could be given as follows.

- To look into the effect of various parameters like voltage, current and flux on losses.
- To study the mathematical modeling of induction motor, and its development.
- Study of different types of loss minimization algorithms, to improve induction motor efficiency.
- In-situ efficiency determination of induction motor through parameter estimation.
- Development and design of loss model controller (LMC).
- Comparing the simulation results when LMC is used with the results obtained when constant flux control technique is used.
- Sensitivity analysis of loss model controller under parameter variation.

1.3 Literature review:

Energy efficiency control of motors is essential one because it is not possible to optimize the efficiency of the motor for every operating point by machine design. This section presents a review of the developments in the field of efficiency optimization control of three phase induction motor. Energy efficient control covers both broad approaches namely, loss model control and search control. Induction motor is a high efficiency electrical machine when working close to its rated speed and torque. However at light loads no balance between copper losses and iron losses results considerable reduction in efficiency. The part load efficiency and power factor can be improved by adjusting the motor excitation in accordance with load and speed. To implement the above objective, the induction motor should be fed through an inverter.

The work first started with the development of induction motor model including iron loss component on dq axis. R.H. Park introduced a new approach to electrical machine analysis. He formulated a change of variable which, in effect, replaced the variables associated with the stator windings of synchronous machine with variables associated with fictitious winding rotating with the rotor. In other words, he transformed, or referred the stator variables to a frame of reference fixed in the rotor. Park's transformations, which revolutionized electrical machine analysis, has the unique property of eliminating all time varying inductances from the voltage equation of the synchronous machine which occur due to electrical circuits in relative motion and electric circuits with varying magnetic reluctance. After R.H. Park, Stanley did noticeable work in the analysis of induction motor in the late 1960s. He showed that the time varying inductances in the voltage equations of an induction machine due to electric circuits in relative motion could be eliminated by transforming the variables associated with rotor windings to variables associated with fictitious stationary windings. In this case, the rotor variables are transformed to a frame of reference fixed in the stator called stator reference frame. After H.C. Stanley, G. Kron introduced a change of variables that eliminated the position or time varying mutual inductances of a symmetrical induction machine by transforming both the rotor variables to a reference frame rotating in synchronism with the rotating magnetic field. This reference frame is commonly referred to as the synchronously rotating reference frame. D.S. Brereton also employed a change of variables that also eliminated the time varying inductances of a symmetrical induction machine by transforming the stator variables to a reference fixed in the rotor called rotor reference frame. This is essentially Park's transformation applied to induction machines.

Kioskeridis and Margaris [3] calculated the total of iron loss, copper loss and stray loss and derived an optimal flux level that minimizes the total loss. They developed loss model based algorithm and induction motor on field oriented scheme. Garcia et al. [4] obtained a loss model after simplifying the induction motor equivalent circuit by deleting leakage inductance in d-q coordinates. The loss model consists of resistors reflecting iron loss, rotor and stator copper losses as a function of stator current i.e. i_{ds} and i_{qs} in the d-q frame. Based on the loss model, a d-axis current level is calculated that minimizes the total loss. Lorenz and Yang [5] took copper and iron loss into account to formulate the loss model. Using an objective function that depends on the drive's loss and includes constraints, they calculated the optimal flux trajectories for the vector control online. Search controllers require input power measurement. Moreira et al. [2]

used the information of third-harmonic components of air gap flux to reduce the d-axis current. Sul and Park [6] proposed an efficiency maximizing technique by defining an optimal slip. The optimal slip is first searched by trial and error, and stored in the microprocessor memory. Then the controlled system is forced to track the optimal slip presented in the lookup table. This technique can be considered as an indirect way to minimize the input power. Kirschen et al. [7] proposed a solution of minimizing the input power by decreasing the flux command in steps. This is a very simple technique, but torque pulsation is unavoidable. Sousa et al. [8] improved the work of Kirschen et al. [7] by adaptively reducing the reference flux current with the aid of fuzzy logic. They solved the torque pulsation problem by applying feed forward compensation. Kim et al. [9] adjusted the squared rotor flux according to a minimum power algorithm based on the Fibonacci search method.

1.4 Organization of dissertation:

The dissertation mainly consists of stepwise study of the induction motor and losses, loss minimization algorithms and design of energy efficient controllers. Mainly the dissertation is divided into six sections.

CHAPTER 1 is a review of previous work done to develop induction motor model and to improve the efficiency of the induction motor.

CHAPTER 2 is discussion of need of induction motor in industrial and house hold application and various losses in induction motor and also explains the effect of various parameters on different types of losses.

CHAPTER 3 is the detailed review of various types of loss minimization algorithms and difference between different types of algorithms.

CHAPTER 4 deals with mathematical modeling of energy efficient controllers, mainly focused on loss model based controller.

CHAPTER 5 deals with in-situ efficiency determination of induction motor (5 hp) through parameter estimation without performing no-load test.

CHAPTER 6 finally sums up the results obtained from Loss Model Control of induction motor drive.

CHAPTER 7 gives final conclusion about work and future scope.

3- Φ Induction Motor and Different Types of Losses in Induction Motor

[This chapter deals with introduction of induction motor and different types of losses. The effect of various parameters like voltage, current and flux on the losses is also discussed.]

2.1 Introduction:

There has been a growing global concern over energy consumption and the environment and high energy efficiency have become one of the most important factors in the development of the products that consume electrical energy [10]. Considering that induction motors (IM) are most widely used in industry, loss minimization of an IM drive requires more attention than ever before. In an effort to improve the efficiency of the motor drive, there have been improvements in the materials, design and construction techniques. However, motor loss is still greatly dependent on control strategies, especially when the motor operates at light load [10].

Now a day's more than 60% of all the electrical energy generated in the world is used by cage induction machines that have been mostly used at fixed speed for more than a century [1].

D.C machines have been used for variable speed applications. In DC machines, mmf axis is established at 90° electrical to the main field axis. The electromagnetic torque is proportional to the product of field flux and armature current. Field flux is proportional to the field current and is unaffected by the armature current because of orthogonal orientation between armature mmf and field mmf. Therefore in a separately excited DC machine, with a constant value of field flux the torque is directly proportional to the armature current. Hence direct control of armature current gives direct control of torque and fast response. Hence they are simple in control and offer better dynamic response inherently. Numerous economical reasons, for instance high initial cost, high maintenance cost for commutators, brushes and brush holders of DC motors call for a substitute which is capable of eliminating the persisting problems in dc motors. Freedom from regular maintenance and a brushless robust structure of the three phase squirrel cage induction motor are among the prime reasons, which brings it forward as a good substitute.

The ac induction motors are the most common motors used in industrial motion control systems, as well as in main powered appliances. Simple and rugged design, low cost and low maintenance are some of the main advantages of 3 phase ac induction motors. Various types of induction motors are available in the market. Different motors are suitable for different application. The speed and torque control of 3 phase induction motors require great understanding of the design and characteristics of these motors.

Static frequency conversion has liberated the induction motor from its historical role as a fixed speed machine. The inherent advantages of adjustable frequency operation cannot be fully realized unless a suitable control technique is employed. The choice of technique is vital in determining the overall characteristics and performance of the drive system. Also the power converter has little excess current capability; during normal operation the control strategy must ensure that motor operation is restricted to the regions of high torque per ampere, thereby matching the inverter ratings and minimizing the system losses. Overload or fault conditions must be handled by sophisticated control rather than over design.

2.2 Losses in Induction Motor:

Losses in induction machines occur in windings, magnetic cores, besides mechanical friction and windage losses. They determine the efficiency of energy conversion in the machine and the cooling system that is required to keep the temperatures under control.

The first classification of losses, based on their location in the IM, includes:

- Winding losses or copper losses – stator and rotor.
- Core losses – stator and rotor.
- Friction and windage losses – rotor.

2.2.1 Copper losses:

Copper losses occur due to resistance of winding. Again these losses are divided into stator and rotor copper losses.

2.2.1.1 Stator copper losses:

The stator copper losses on a non sinusoidal supply are proportional to the square of total rms current. If R_1 is the stator resistance per phase, the total stator copper loss is,

$$P_{scu} = 3I_{rms}^2 R_1$$

Or

$$P_{scu} = 3(I_1^2 + I_{har}^2)R_1(\omega) \quad 2.1$$

Where, the second term represents the harmonic copper loss. It has been found that the harmonic current also increases the fundamental component, due to an increase in the magnetizing current. The magnetizing current increases because of the saturation of the leakage flux paths because of harmonics fluxes.

2.2.1.2 Rotor copper losses:

For large ac motors there is an increase in stator resistance with frequency which depends on the shape, size and disposition of the conductors in the stator slots. However the skin effect is much more pronounced in the cage rotor, which exhibits a significant increase in resistance at harmonic frequencies particularly in case of deep bar rotors. In motors, the fifth harmonic mmf rotating backward and the seventh harmonic mmf rotating forward will induce rotor currents at 6 times fundamental frequency. Similarly rotor currents at 12 times fundamental frequency are induced because of eleventh and thirteenth harmonic mmf. The rotor resistance is much greater than the dc value. The actual increase depends on the geometrical shape of conductor cross section and rotor slot in which it is placed. In general, for k^{th} harmonic the rotor copper loss is

$$P_{rcu k} = 3I_{2k}^2 R_{2k} \quad 2.2$$

I_{2k} is the k^{th} harmonic rotor current. Rotor leakage reactance reduces considerably due to skin effect, thus a lower value of per unit reactance should be taken, which should be approximately 80 to 90% of rated value.

2.2.2 Core losses:

In general, core losses arise both due to induced currents in the core as well as the hysteresis characteristics of the core material. If the magnetic field set up in ferromagnetic core is time varying, the field will induce a voltage in the core and thus cause current flow within the core itself. Due to the finite resistance of the core material, a resultant power loss occurs. These losses can be modelled in terms of hysteresis and eddy current losses and are given by,

$$P_h = K_h f \Phi_m^2 \quad 2.3$$

$$P_e = K_e f^2 \Phi_m^2 \quad 2.4$$

where, P_h – hysteresis loss

P_e – eddy current loss

K_h – hysteresis coefficient given by material and design of motor

K_e – eddy current coefficient given by material and design of motor

f – fundamental frequency of stator voltage

Φ_m – mutual flux or air-gap flux.

The total core loss P_{cs} is determined by combining equations 2.3 and 2.4,

$$P_{cs} = P_h + P_e = K_h f \Phi_m^2 + K_e f^2 \Phi_m^2 \quad 2.5$$

The rotor core loss, P_{cr} is calculated by using equation 2.5, but with slip frequency instead of stator frequency.

$$P_{cr} = K_h s f \Phi_m^2 + K_e (s f)^2 \Phi_m^2 \quad 2.6$$

where s - slip

Total core loss at fundamental frequency is

$$P_c = P_{cs} + P_{cr} = \left[K_h \left(\frac{1+s}{f} \right) + K_e (1+s^2) \right] f^2 \Phi_m^2 \quad 2.7$$

Where P_c - total core loss of the motor

As mutual flux Φ_m is related to air gap voltage V_m and core coefficient K_c as

$$\Phi_m = \sqrt{K_c} \frac{V_m}{f} \quad 2.8$$

Equation 2.7 can be rewritten as,

$$P_c = K_c \left[K_h \left(\frac{1+s}{f} \right) + K_e (1+s^2) \right] V_m^2 \quad 2.9$$

The equivalent core loss resistance R_m can be determined by,

$$R_m = \frac{V_m^2}{P_c} = \frac{1}{K_c \left[K_h \left(\frac{1+s}{f} \right) + K_e (1+s^2) \right]} \quad 2.10$$

With the consideration of harmonics, assuming the coefficients K_h and K_e remain same at harmonic frequency, and since harmonic slip $S_n = 1$, the equivalent core loss resistance R_{mn} at harmonic frequency f_n can be obtained by,

$$R_{mn} = \frac{0.5}{K_c \left(\frac{K_h}{f_n} + K_e \right)} \quad 2.11$$

If we simplified the above equation further by considering $K_h = K_e = K_{he}$

$$R_{mn} = \frac{0.5f_n}{K_c K_{he} (1 + f_n)} \quad 2.12$$

By observing the equation 2.12,

$$R_{mn} \propto \frac{f_n}{1 + f_n}$$

This means change in core loss resistance with change in frequency is not much considerable, and we can keep the core loss resistance value almost independent of frequency.

2.2.3 Stray load loss:

The stray losses are high frequency losses in the induction motor caused by space harmonics in the air-gap flux. Magneto Motive Force (MMF) of the motor load currents, which divert some of the no load magnetic flux into leakage paths, thereby creating flux pulsations and eddy current losses in the laminations, conductors and adjacent metal parts. Stray losses can be represented by a group of losses and empirical equations can be used to evaluate them which require the knowledge of machine dimensions, type of core material, lamination thickness, winding geometry etc.

The stray losses can be modelled in a way similar to that used for core loss modelling. The stator stray loss per phase at harmonics frequency f_n can be given as,

$$P_{str} = K_{str} \left[\frac{K_h}{f_n} + K_e \right] V_{sn}^2 \quad 2.13$$

Where, P_{str} – stray load loss at harmonic frequency

K_{str} – stray loss constant at harmonic frequency

V_{sn} – voltage across the stator leakage inductance at harmonic frequency

The losses at harmonic frequency can be represented by an equivalent resistance R_{str} in parallel with leakage inductance as,

$$R_{str} = \frac{1}{K_{str} \left[\frac{K_h}{f_n} + K_e \right]} \quad 2.14$$

The expression of voltage across the stator leakage inductance, V_s is

$$V_s = 2\pi f L_s I_s \quad 2.15$$

For the fundamental frequency, stray loss can be modelled as

$$P_{str} = K_{str} [K_h f + K_e f^2] I_s^2 \quad 2.16$$

where, P_{str} – stray load loss at fundamental frequency

V_s – voltage across the stator leakage inductance at fundamental frequency

I_s – stator fundamental current

f – fundamental frequency

The equivalent resistance R_{str} can be represented in series with the stator leakage reactance as given by

$$R_{str} = K_{str} [K_h f + K_e f^2] \quad 2.17$$

The simplified equation for the stray load losses is given by,

$$P_{str} = K_{str} f^2 I_r'^2 \quad 2.18$$

Where, I_r' – rotor current referred to stator.

2.2.4 Mechanical losses:

The main reasons of mechanical losses appearing in the induction motor are friction and windage losses. These losses are relatively a small percentage of the total motor losses and are separated by the four components. These are friction loss in the bearing, windage loss of outside fan, friction losses of rotor and windage losses of internal fans and finally friction power loss of V – ring seals. Normally, total mechanical losses are approximated as,

$$P_{mech} = C_{fw} \omega_r^2 \quad 2.19$$

where, ω_r – speed of the rotor

C_{fw} – mechanical power loss coefficient

The total loss at both fundamental and harmonic frequency, P_{loss} in the induction motor considering conductor losses, iron losses, stray losses, mechanical losses is given by,

$$P_{\text{loss}} = 3(I_1^2 + I_{\text{har}}^2)R_1(\omega) + 3I_{2k}^2 R_{2k} + \left[K_h \left(\frac{1+s}{f} \right) + K_e (1 + s^2) \right] f^2 \Phi_m^2 + K_{\text{str}} f^2 I_r'^2 + C_{\text{fw}} \omega_r^2 \quad 2.20$$

By observing the above equation, loss in induction motor is a function of load current or load torque, speed, air-gap flux, and frequency and can be written as,

$$P_{\text{loss}} = f(T_l, \Phi_m, f) \quad 2.21$$

2.3 Efficiency maximization:

The main losses, about 80% of the total losses, are copper (stator + rotor) and iron losses. In a conventional machine, operation under rated conditions is highly efficient. This results from a favourable balance between copper and iron losses. Under these conditions efficiencies of 74 to 92% are usual for machines rated between 1 to 100 hp. However, there are many applications which require adjustable torque and/or speed [11]. A torque and/or speed far from the rated operating point causes a notorious IM efficiency drop. This is due to the imbalance between iron and copper losses. Under these circumstances, it is not possible to increase the efficiency by the improvement of the machine design. Several controllers allow efficiency optimization when the IM works with light loads. Several strategies using different variables to minimize losses have been proposed. Some algorithms use power factor stator current, stator power, volt/Hertz rate, rotor flux, voltage input, or slip as independent control variables. Although different variables have been controlled, in all these methods the efficiency improvement is always achieved by indirectly controlling the balance between copper and iron losses. The mechanism that permits the electromagnetic loss minimization acts as follows: Electromagnetic torque is proportional to the vector product of the magnetic flux and rotor current. It is thus possible to obtain the same torque with different combinations of flux and current values. For a given torque, the iron loss can be minimized by using the minimum possible flux. This also minimizes the stator copper loss component due to the magnetizing current. On the other hand, to create the required torque with less magnetizing flux, the rotor current must be increased by increasing the stator current and consequently the total copper losses. By a proper adjustment of the magnetic flux, an appropriate balance between copper and iron losses can be achieved to minimize the electromagnetic losses.

2.4 Conclusion:

Induction motor is a high efficiency electrical machine when working close to its rated speed and torque. This results from a favourable balance between copper and iron losses. A torque or speed far from the rated operating point causes a notorious IM efficiency drop. This is due to the imbalance between iron and copper losses. Under these circumstances, it is not possible to increase the efficiency by the improvement of the machine design. Several control methods have been proposed to minimize losses when the IM works with light loads which will be discussed in next chapter.

Optimal Controllers for Induction Motor Drive

[This chapter is discussion of various types of efficiency optimization techniques like search technique, loss model based technique and difference between different types of efficiency optimization techniques.]

3.1 Introduction:

Several operation schemes have been proposed by many researchers to choose flux level in induction motor for attaining maximum efficiency. In low-frequency operation, core loss (hysteresis and eddy current loss) is rather low compared with copper loss. As the speed goes up, however, the contribution of the eddy current loss increases and finally becomes dominant. Hence, the optimal combination of d-axis and q-axis currents varies, depending on the required torque and speed. The techniques allowing efficiency improvement can be divided into two categories:

- (1) Loss-model-based approach, which consists of computing losses by using the machine model and selecting a flux level that minimizes these losses.
- (2) Power-measure-based approach, also known as search controllers (SCs), in which the flux (or its equivalent variables) is decreased until the electrical input power settles down to the lowest value for a given torque and speed.

Kioskeridis and Margaritis [3] calculated the total of iron loss, copper loss and stray loss and derived an optimal flux level that minimizes the total loss. Garcia et al [4] obtained a loss model after simplifying the induction motor equivalent circuit by deleting leakage inductance in d–q co-ordinates. The loss model consists of resistors reflecting iron loss, rotor and stator copper losses as a function of stator current i.e. i_{ds} and i_{qs} in the d–q frame. Based on the loss model, a d-axis current level is calculated that minimizes the total loss. Lorenz and Yang [5] took copper and iron loss into account to formulate the loss model. Using an objective function that depends on the drive's loss and includes constraints, they calculated the optimal flux trajectories for the vector control online. Search controllers necessitate the use of input power measurement. Moreira et al [2] used the information of third-harmonic components of air gap flux to reduce the

d-axis current. Sul and Park proposed an efficiency maximizing technique by defining an optimal slip. The optimal slip is firstly searched by trial and error, and stored in the microprocessor memory. Then the controlled system is forced to track the optimal slip presented in the lookup table. This technique can be considered as an indirect way to minimize the input power. Kirschen et al [7] proposed a solution of minimizing the input power by decreasing the flux command in steps. This is a very simple technique, but torque pulsation is unavoidable. Sousa et al improved the work of Kirschen et al by adaptively reducing the reference flux current with the aid of fuzzy logic. They solved the torque pulsation problem by applying feed forward compensation. Kim et al [12] adjusted the squared rotor flux according to a minimum power algorithm based on the Fibonacci search method. The torque ripple is not generated in this configuration, since the speed and rotor flux are decoupled by means of nonlinear control. In model-based loss-minimization algorithms (LMAs), the leakage inductance of stator and rotor are usually neglected to simplify the loss model and minimization algorithm. However, with this simplified model, the exact loss minimization cannot be achieved, especially for high-speed operation of EV motors, since a large voltage drop across the leakage inductance is neglected. To find the loss expression from the full loss model is a very complex and weary job. In this paper, a simplified induction motor model with iron loss is developed. Then the validity of the model is examined by computation results. Further, current and voltage constraints are considered when generating the optimal flux level for loss minimization.

There are three types of efficiency optimization controllers for induction motor:

- (a) Loss model controller (LMC)
- (b) Search controller (SC) and
- (c) Hybrid controller

3.2 Loss model controller (LMC):

Loss model controller measures the speed and stator current and determines optimal air gap flux through the loss model of the motor. Control algorithm may be scalar in inner part [13]. In scalar control technique, variables are controlled in magnitude only whereas in vector control, variables are controlled in magnitude and phase. The complex induction motor can be modeled as DC motor by performing simple transformation in the vector control scheme. One advantage of loss model controller is that no delay in calculation of optimal flux and drive performances but

time delay occurs in case of search control due to the search. Artificial intelligence controllers like ANN, fuzzy, PSO, GA can also be used for finding optimal flux level with minimum time. The exact values of machine parameters including their variations due to core losses and main inductance flux saturation are required in this approach. Different variables like slip speed, rotor flux, excitation current, voltage can be used to minimize losses in IM.

3.2.1 Scalar Controlled Drives:

The behavior of an ac induction motor drive is described by three independent variables- the speed, the terminal voltage, the terminal frequency and the parameters of the motor and its power supply [13]. At any operating point characterized by the speed and torque, an optimal flux (in other words, ratio of voltage and frequency) can be found that meets the requirement of the operating point and minimizes the overall losses.

(a)Conventional Controllers:

A loss model controller with detailed analysis for minimizing the losses in scalar controlled induction motor is presented and suggested that the air gap flux is always kept greater than 0.3 pu independently on LMC command. This is because very low flux creates more motor currents and disturbs torque and finally losses will be more. Rated flux operation is essential during transient to maintain good dynamics. The procedure here is based on optimal slip control of current source inverter fed induction motor. First, the optimal slip is searched by trial and error with the help of loss model and the results are tabulated in microprocessor memory. Then the motor is operated at optimal efficiency by simply tracking the optimal slip given in the table. The span of the optimal slip with respect to torque is high in case of lower speed rated motors. The variables, input voltage and frequency are considered to optimize the motor efficiency. It should be noted that the flux level can be adjusted to get maximum efficiency without considering inverter losses in small drives less than 10 kW; but the effect of inverter losses in medium size (10-1000 kW) drives is significant.

(b)AI and NIA Based Controllers:

Many recent developments in science, economics and engineering, demand numerical techniques for searching global optima to corresponding optimization problems. As we discussed earlier, the effect of motor parameter variations has been focused and GA is used to search motor parameter to avoid error in the loss model. Then optimum voltage and frequency arranged as table for the

energy saving controller. The inputs to the NN are torque, speed and rotor resistance of the IM and the output is the optimum rotor flux to minimize total losses. Particle swarm optimization (PSO) is also a searching tool, used to find the optimal value of variables for which the objective is maximum/minimum. ANN is used for implementing optimum variables in the controllers. PSO is used to adjust proportional –integral- differential controller gains and get less torque and speed ripples in the drive.

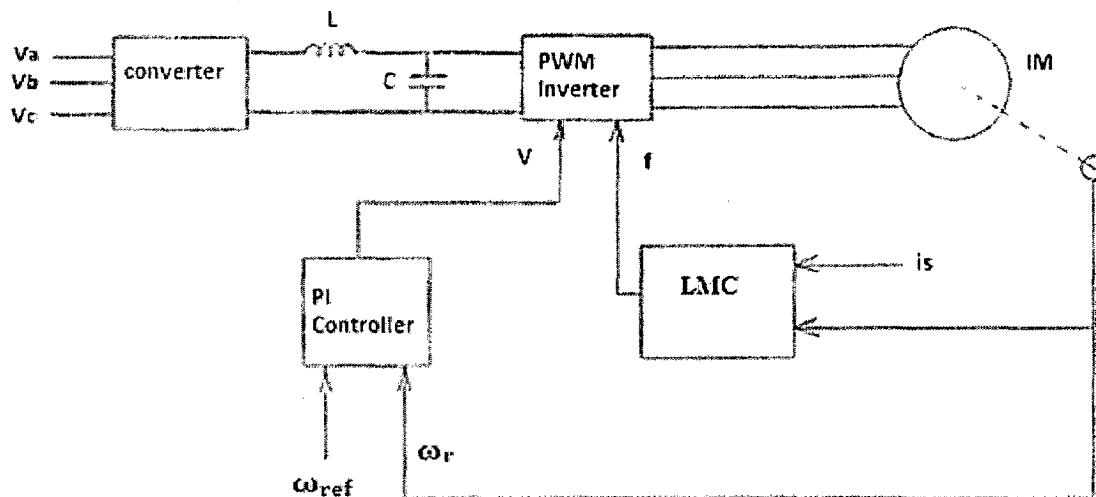


Fig.3.1 Scalar controlled drive using LMC

3.2.2 Vector Controlled Drives:

In vector control, the variables are considered in magnitude and phase [13]. This technique of control needs more calculation than scalar control. The field oriented controller (FOC) generates the required reference currents based on the reference torque.

(a) Conventional Controllers:

Generalized d-q loss (vector) model including core saturation effects is presented in and optimized IM, permanent magnet synchronous motor, direct current motor, synchronous reluctance motor through optimal excitation current (i_{ds}). It was concluded that minimum losses are reached when d axis power losses equal to q axis power losses. Parameter variation effects during loss minimization in induction motor through the simple IM loss motor including iron losses must be studied to achieve minimum electromagnetic loss by proper adjustment of magnetic flux. The procedures to get minimum energy are that derive the steady state values of currents and fluxes for the given load and design the steady state feedback control based on

lyapunov. Then implement the steady state values in real time and finally get good torque stability under minimum energy operation of IM.

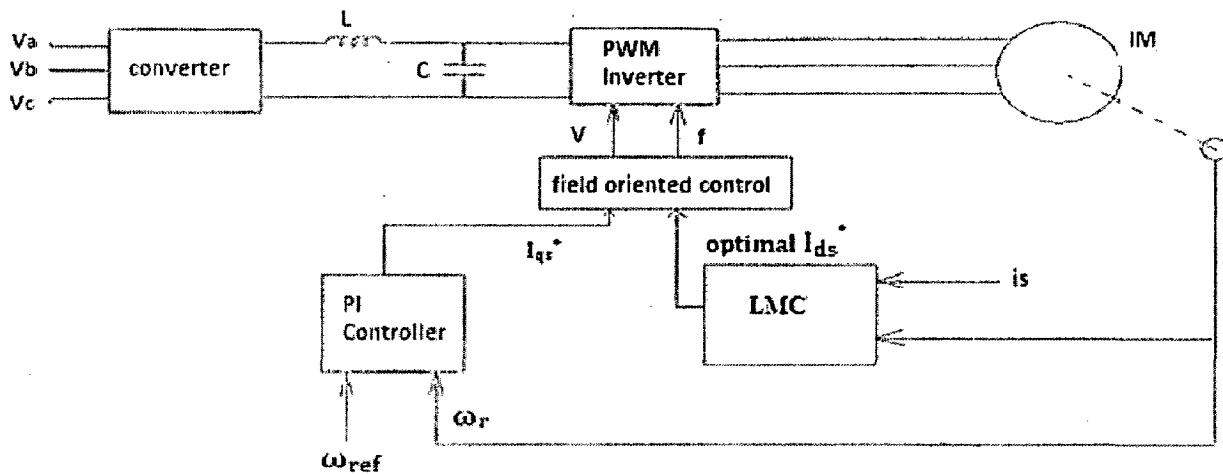


Fig.3.2 Vector controlled drive using LMC

(b)AI Based Controllers: A hybrid technique, GA-PSO based vector control of induction motor for loss minimization as well as torque control is proposed by D.H. Kim. PSO is used for mutation process of GA so that the learning efficiency of GA is improved. Floating point GA is applied for minimizing IM losses through flux adjustment. Basic GA is used to identify rotor time constant from the error between motor and commanded stator currents, which helped on-line adjustment of slip angular speed. Optimum flux producing current and corresponding efficiency are focused by using neural network. Change in core loss resistance due to flux and frequency have been taken into account.

3.3 Search Controller:

Search control (SC) does not require the knowledge of the motor loss model for implementing optimization controllers. This controller measures the input power of the machine drive regularly at fixed interval and searches optimal flux value which results in minimum power input or stator current for the given values of speed and torque [13]. Torque ripple is always present in SC due to the oscillations in the air gap flux. The advantages of SC control in induction motor efficiency optimization are as follows

(a) If the power input is measured on the source side of the rectifier, the minimization is not restricted to the motors but affects the entire system and thus reduces the total amount of energy consumed.

(b) Since the source voltage and current waveforms have a much smaller harmonic content than the corresponding motor waveforms, the power measurement is more accurate and easier to obtain.

(c) Insensitive to parameter variation in the motor due to thermal and core saturation affects the performance.

3.3.1 Scalar Controlled Drives: When stator current used as variable, its minimum can be more easily detected than the input power. Stator current leads more loss reduction and less torque ripple due to the absence of oscillation in the air gap flux; input to the drive is smaller in stator current minimization than the power input minimization. Minimum power input to the drive is achieved by adjusting inverter input frequency. Voltage adjustment is carried out according to losses for minimum power input and the second controller changes the frequency to correct rotor speed losses caused by voltage drops. The third controller produces an initial commanded frequency which compensates the variation in slip with changing load and speed.

3.3.2 Vector controlled Drives: In this Flux producing current (i_{ds}) was considered as variable. Torque producing current (i_{qs}) is also adjusted in accordance with i_{ds} to avoid deterioration in the torque. Convergence of program (reduces flux step by step until input power is minimized) and the minimization process depends on the motor time constant. Thus longer time for high rated motor and shorter time for larger rated slip. Moreover fast convergence produces more ripples in the torque. The squared rotor flux is adjusted until the measured input power reaches to minimum. The controller depends on rotor resistance and its variations are taken into account. Three indirect vector control schemes namely, stator flux field orientation, rotor flux field orientation and air gap flux field orientation are used for optimizing IM torque and efficiency.

3.3.3 AI and NIA Based Controllers: Loss minimization is achieved during transient state by adjusting flux level using fuzzy logic. Voltage is considered as a controlling variable. For both steady state and transient state, fuzzy logic is used to optimize motor efficiency. Fuzzy logic is used to decrement flux until the drives settle down at minimum input power. But as the speed

or torque command changes, the efficiency optimization using fuzzy is abandoned and the rated flux is established to get the best transient performance. Feed forward torque compensator is used to reduce torque pulsation.

3.3.4 Both LMC and Search Control: Both LMC and SC are used to analyze induction motor efficiency optimization. The developed controller ensures to retain good features of both the LMC and SC, while eliminating their major drawbacks. Therefore, slow convergence (drawback of SC) and parameter variation (drawback of LMC) are eliminated. LMC is more appropriate in FOC because optimal flux can be imposed in a short time where as search controls vary the flux continuously which produce more oscillations in the torque.

3.4 Loss Model Controller vs. Search Controller:

Both the methods minimize the motor losses but in different ways. The Loss Model Controller is a feed-forward approach, which calculates the optimum set of variables of the machine, depending on the optimization (maximize or minimize) of an objective function, defined using the machine parameters. The objective function is usually an analytical expression representing either the loss or the efficiency or the total power input. The optimum variable may be the operating flux of the machine or the slip frequency or some other variables depending on the objective function. The fast calculation for the determination of the optimum variables is the merit of this method. However, the demerits are

- (a) The method is dependent on machine parameters, hence if the approach is not based on on-line estimation of the parameters then it is likely that the method may offer only sub-optimal solution if the parameters of the machine change.
- (b) The stray load loss and the mechanical loss also are not strictly constant and an exact modelling of these losses is very complicated.
- (c) Inclusion of the whole drive system including the power electronic interface requires modelling of the same, which again makes the method more complicated. The Search technique on the other hand depends on the exact measurement of the input power and minimization of the same through a suitable approach. Thus the method does not have the problems of the LMC as outlined.

3.5 Conclusion:

Different types of efficiency optimization controllers: loss model controller (LMC) and search controller (SC) have been discussed in this chapter. The difference between different efficiency optimization techniques is also studied. The suggested method can be easily implemented with digital techniques like DSP and only the stator current measurement is required. Therefore, the method does not considerably affect the cost of the drive. The suggested method can be used in both open and closed speed loop drives but closed loop drive gives better performance compared to open loop drive.

Modeling of Energy Efficient Controllers

[This chapter deals with mathematical modeling of energy efficient controllers, mainly focused on loss model based controller.]

4.1 Introduction:

In previous chapter different types of optimization algorithms like loss model technique, search technique and hybrid technique are discussed. Mathematical model gives clear idea of, how the losses are minimized, and what parameters are needed for implementing loss minimization algorithms. This chapter begins with the mathematical modeling of loss model based controller.

4.2 Modelling of LMC:

An equivalent circuit for IM can be varied by the different choice of flux linkage constant [10]. In this paper, we utilize an equivalent circuit referenced to the rotor magnetizing current by defining the rotor flux as

$$\psi_r = L_m \cdot i_r \quad 4.1$$

An iron loss resistor is added in parallel to the magnetizing inductance in a reference frame fixed to the rotor magnetizing current as shown in Fig.4.1 and the d-axis has been aligned in the direction of the magnetizing current i_m as shown in Fig.4.2.

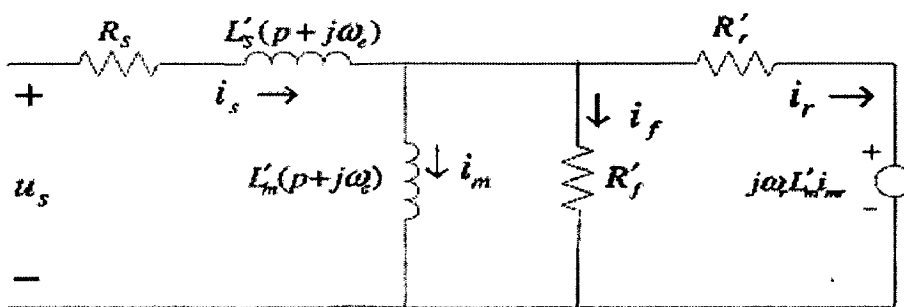


Fig.4.1 Space vector equivalent circuit in a rotor-flux-oriented reference frame including an iron loss resistor

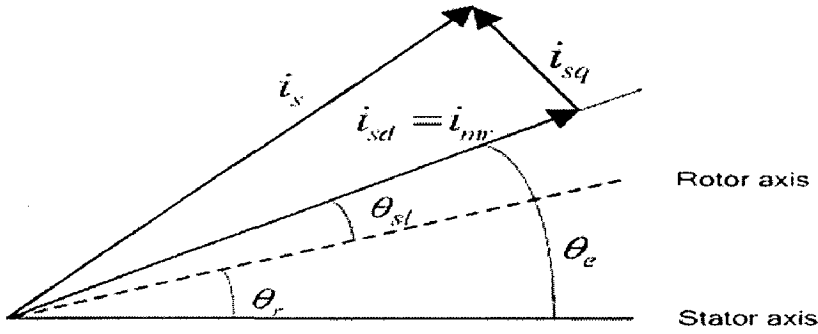


Fig.4.2 Phasor diagram of equivalent circuit and rotor field angle definition

Defining the differential operator $p = d/dt$, the space vector motor model in a rotating reference frame is given by

$$u_s = R_s i_s + p L'_s i_s + j \omega_e L'_s i_s + p L'_m i_m + j \omega_e L'_m i_m \quad 4.2$$

$$\begin{aligned} i_s &= i_m + i_f + i_r \\ &= i_m + (p + j \omega_e) \frac{L'_m}{R'_f} i_m + (p + j(\omega_e - \omega_r)) \frac{L'_m}{R'_r} i_m \end{aligned} \quad 4.3$$

Where $\omega_e = \frac{d\theta_e}{dt}$ is the electrical angular speed of the rotor flux and $\omega_r = \frac{d\theta_r}{dt}$ is the electrical rotor speed. For the rotor-flux-orientation control scheme

$$\begin{aligned} u_s &= u_{sd} + j u_{sq}, \quad i_s = i_{sd} + j i_{sq}, \quad i_m = i_{md} + j i_{mq} \\ i_{mq} &= 0, \quad i_{md} = i_{mr} = \text{constant} \end{aligned} \quad 4.4$$

We obtain,

$$u_{sd} = R_s i_{sd} + p L'_s i_{sd} - \omega_e L'_s i_{sq} + p L'_m i_{mr} \quad 4.5$$

$$u_{sq} = R_s i_{sq} + p L'_s i_{sq} + \omega_e L'_s i_{sd} + \omega_e L'_m i_{mr} \quad 4.6$$

$$i_{sd} = i_{mr} + p \left(\frac{L'_m}{R'_f} + \frac{L'_m}{R'_r} \right) i_{mr} \quad 4.7$$

$$i_{sq} = \omega_e \frac{L'_m}{R'_f} i_{mr} + (\omega_e - \omega_r) \frac{L'_m}{R'_r} i_{mr} \quad 4.8$$

Let $R_t = R_r // R_f$

From equation (4.7) the magnetizing current can be expressed by:

$$i_{mr} = \frac{1}{1+p\left(\frac{L'_m}{R'_r} + \frac{L'_m}{R'_f}\right)} i_{sd} = \frac{1}{1+p\frac{L'_m}{R'_r}} i_{sd} \quad 4.9$$

From equation (4.8) the slip speed can be derived as,

$$\omega_{slip} = \frac{R'_r}{L'_m} \frac{i_{sq}}{i_{mr}} - \omega_e \frac{R'_r}{R'_f} = \frac{R'_r}{L'_m} \frac{i_{sq}}{i_{mr}} - \omega_r \frac{R'_r}{R'_f} \quad 4.10$$

Torque developed:

From equation (4.10) developed torque can be written as

$$\begin{aligned} T_e &= \frac{3}{2} Z_p \frac{(L'_m i_{mr})^2}{R'_r} \omega_{slip} \\ &= \frac{3}{2} Z_p L'_m i_{sq} i_{mr} - \frac{3}{2} Z_p \frac{(L'_m i_{mr})^2}{R'_f} \omega_e \end{aligned} \quad 4.11$$

In the steady state of the motor model in Fig.4.1, there is no leakage inductance on the rotor side and the sum of rotor current i_r and the iron current i_f is perpendicular to the magnetizing current, i_{mr} . Hence the circuit illustrates decomposition of the stator current i_s into the rotor flux oriented components: $i_{sd}=i_{mr}$ which forms the flux ψ_r , and $i_{sq}=i_f+i_r$ which is related to control the torque developed by the motor. From the motor model (equations (4.5) to (4.8)) the steady-state IM equivalent circuit in a field-oriented frame can be shown as in Fig.4.3. d-axis equivalent circuit can easily be derived from equations (4.5) and (4.7) and q-axis equivalent circuit can easily be derived from equations (4.6) and (4.8) considering that the terms with differentiation will be zero in steady state.

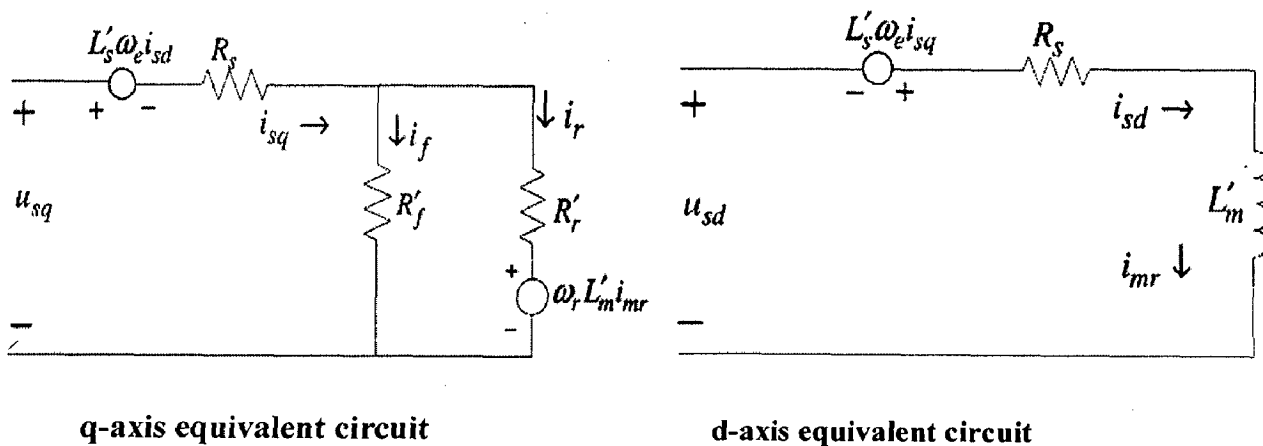


Fig.4.3 Steady state equivalent circuit of IM on d, q axes respectively

In the development of the loss model, a typical method for model simplicity used in previous research is to ignore the leakage inductance. The decomposition feature of the proposed motor model makes the derivation of the loss model more straightforward without any assumption for model simplicity. Stator copper, rotor copper and iron losses dominate the overall power loss compared to stray, friction, windage and converter losses. In the current work, stray, friction, windage and converter losses are neglected. From Fig.4.3, the total loss is given by

$$P_{total} = P_{cus} + P_{cur} + P_{iron}$$

$$P_{total} = R_s (i_{sd}^2 + i_{sq}^2) + R_f' (i_{sq} - i_r)^2 + R_r' i_r^2 \quad 4.12$$

P_{cus} = Stator Copper loss

P_{cur} = Rotor Copper loss

P_{iron} = Iron loss

$$i_r = i_{sq} - i_f = i_{sq} - \frac{R_r'}{R_f'} i_r - \omega_r \frac{L_m'}{R_f'} i_{sd} \quad 4.13a$$

Then,

$$i_r = \frac{R_f}{R_f + R_r'} i_{sq} - \omega_r \frac{L_m'}{R_f + R_r'} i_{sd} \quad 4.13b$$

Substituting i_r from equation (4.13) into (4.12) yields,

$$P_{total} = R_d i_{sd}^2 + R_q i_{sq}^2 \quad 4.14$$

Where,

$$R_q = R_s + \frac{R_f' R_r'}{R_f' + R_r'} \quad 4.15$$

$$R_d(\omega_r) = R_s + \frac{L_m'^2}{R_f + R_r} \omega_r^2 \quad 4.16$$

The developed electrical torque can be expressed in different ways. From Fig.4.3 and equation (4.13), torque can be expressed as,

$$T_e = \frac{3P}{2} L_m' i_{mr} i_r$$

$$= \frac{3P}{2} L_m' \left(\frac{R_f'}{R_f' + R_r'} \right) i_{sq} i_{mr} - \frac{3P}{2} \frac{(L_m' i_{mr})^2}{R_f' + R_r'} \omega_r \quad 4.17$$

By utilizing equation (4.10) torque can also be written as,

$$\begin{aligned}
T_e &= \frac{3P}{2} \frac{(L'_m i_{mr})^2}{R'_r} \omega_{slip} \\
&= \frac{3P}{2} L'_m i_{sq} i_{mr} - \frac{3P}{2} \frac{(L'_m i_{mr})^2}{R'_f} \omega_e
\end{aligned} \tag{4.18}$$

If the second expression from equation (4.10) is used in equation (4.18), the torque expression (4.18) becomes the same as (4.17). The second term of the right side of (4.18) represents the loss in developed torque due to iron loss resistance. Since $R'_f \gg R'_r$ and $(R'_f + R'_r) \gg (L'_m i_{mr})^2$ torque equations (4.17), (4.18) can be approximated as,

$$T_e \approx \frac{3}{2} \frac{P}{2} L'_m i_{sq} i_{mr} = K_t i_{sq} i_{mr} \tag{4.19}$$

Where,

$$K_t = 3/2 Z_p L'_m$$

Then in steady state,

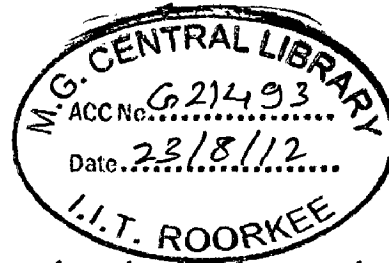
$$i_{sq} = T_e / K_t i_{sd} \tag{4.20}$$

The differentiation of the loss expression equation (4.12) with respect to i_{sd} for a constant torque gives the following relation between i_{sq} and i_{sd} .

$$\frac{dP_{total}}{di_{sd}} = 2R_d i_{sd} + 2R_q i_{sq} (i_{sd}) \frac{di_{sq}(i_{sd})}{di_{sd}} \tag{4.21}$$

Putting equation (4.19) into equation (4.21) leads to,

$$\frac{dP_{total}}{di_{sd}} = 2R_d i_{sd} - 2R_q \frac{i_{sq}^2}{i_{sd}} = 0 \tag{4.22}$$



This result implies that the motor losses reach a minimum when the d and q axes losses are equal. Thus, an optimum level of magnetizing current for minimum loss is given by

$$i_{mr_opt} = \sqrt{\frac{R_q}{R_d(\omega r)}} i_{sq} \tag{4.23}$$

and

$$K = \sqrt{\frac{R_q}{R_d(\omega r)}} = \frac{i_{mr_opt}}{i_{sq}}$$

is the loss factor. Based on the above algorithm, the block diagram of the closed loop vector control scheme of IM drive is shown in Fig.4.4.

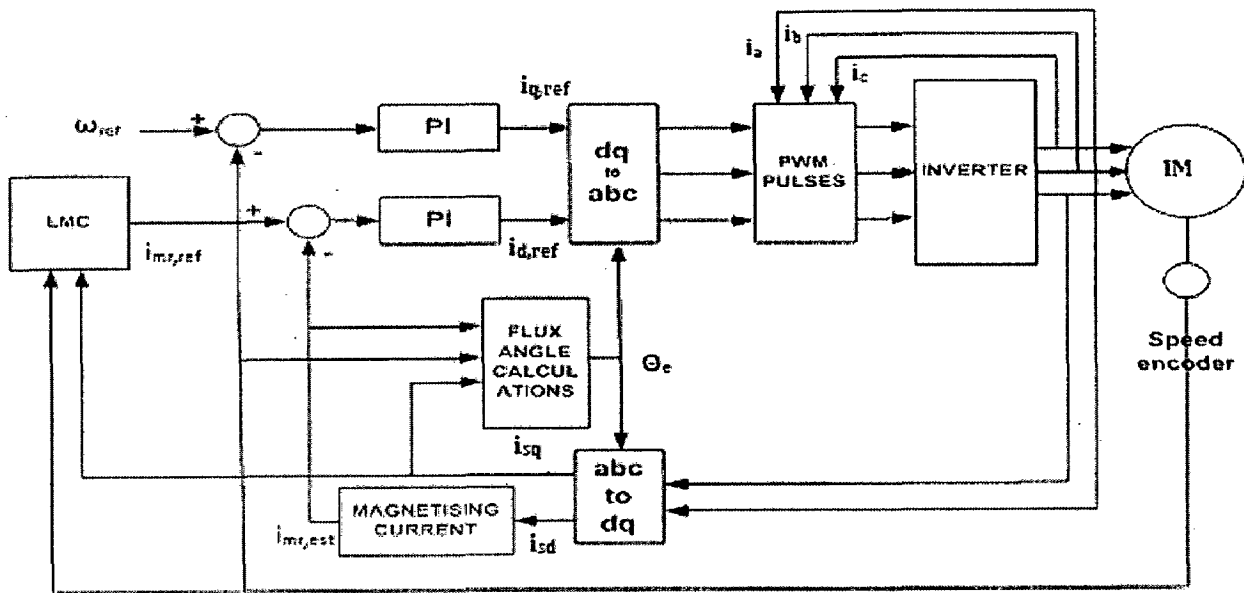


Fig.4.4 Overall block diagram of proposed loss model based induction motor drive

4.3 Modelling of search controller:

In search control method, which does not require the knowledge of the motor loss model, DC link or input power of the machine drive is measured regularly at fixed intervals and optimal flux producing current or flux value is searched which results in minimum power input or stator current of the motor for the given values of speed and torque. Once DC link power is minimized the adjustment of flux is stopped and the current flux is maintained and given to field oriented control as flux current command.

Ramp search method:

It is well known fact that oscillation in the flux producing current around its optimal value causes undesirable torque pulsations [11]. Furthermore, many of the search techniques reported so far contain the risk of too much reduction in flux giving rise to stability problem. Usually, this is checked by putting a minimum limit of the flux. But the problem is reaching the minimum limit during the process of search as it may cause early termination of the search routine, if not properly taken care. To avoid such problems ramp search can be used in the SC control which is shown Fig.4.5.

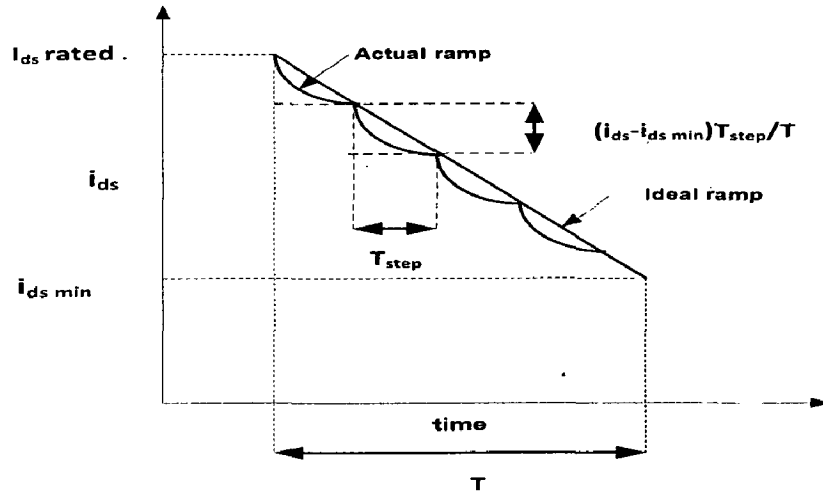


Fig.4.5 Ramp search method

In this type of search control, variable is decreased from its rated value in small steps and corresponding dc link power shows an upward trend. When subsequent magnitude of dc link power is higher, the search is stopped and the control variable is restored to the earlier step value and the optimum condition is thus reached. Referring to Fig.4.5, searching algorithm starts at rated value of flux reference and proceeds with small step towards a preset minimum flux reference in a total time of T sec. Slope of the ramp is given by,

$$(i_{ds(rated)} - i_{ds(min)})/T$$

Current reduction in each step is calculated by

$$\frac{(i_{ds(rated)} - i_{ds(min)}) * T_{step}}{T}$$

The main advantage of this method of search is that it is fairly independent of both the $i_{ds(min)}$ and step time. The DC link power which contains ripples and noise should be allowed to settle down to the steady value after each of step change of flux current command. On the other hand, in this method the optimum magnitude of the flux current command is considered integral number of steps away from the initial value. Thus, a large step size may not converge to the real optimal condition. All these indicate that a proper selection of step size is essential for better response of this method.

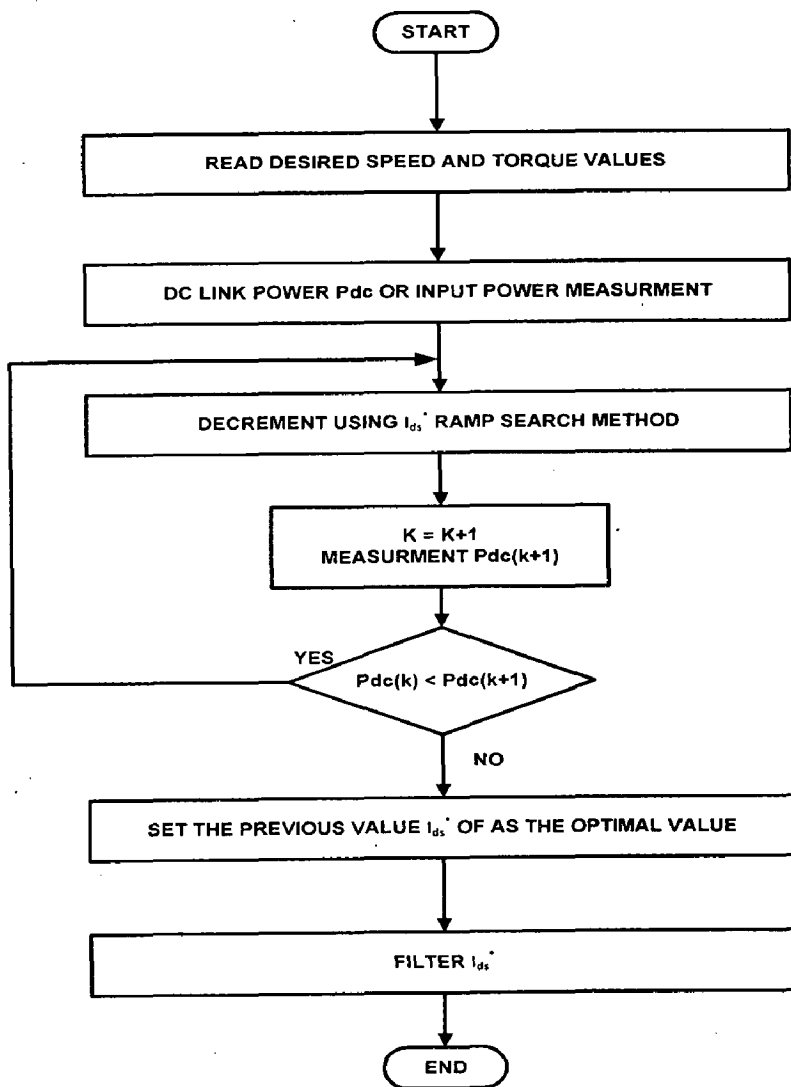


Fig.4.6 Flow chart of Search controller

4.4 Conclusion:

The suggested method can be easily implemented either with digital techniques like dsp, and only the stator current measurement is required. Therefore, the method does not considerably affect the cost of the drive. The suggested method can be used in both open and closed speed loop drives but closed loop drives gives better performance compared to open loop drives.

In-situ Efficiency Determination of Induction Motor through Parameter Estimation

[This chapter deals with efficiency determination of induction motor (5 hp) without performing no-load test. Results are compared with physical efficiency measurement method. The error between estimated and actual efficiencies is found for different objective functions and for different standards.]

5.1 Introduction:

The performance of LMC controller is based on the accuracy of induction motor parameters. Induction motor parameter varies with temperature. The exact knowledge of some of the induction motor parameters is very important to implement efficient control schemes and its in situ efficiency determination. These parameters can be obtained by no-load test that is not easily possible for the motors working in process industries where continuous operation is required. Here, particle swarm optimization is used for in situ efficiency determination of induction motor (5 hp) without performing no-load test. Results are compared with physical efficiency measurement method. The error between estimated and actual efficiencies is found for different objective functions and for different standards.

Many nonlinear programming techniques like the Newton-Raphson technique, cyclic method, Hook, Jeeves, and Rosenbrock methods have been applied to parameter estimation and hence efficiency determination of induction motors. The optimum determined by the Newton-Raphson technique depends heavily on the initial guess of the parameter, with the possibility of a slightly different initial value, causing the algorithm to converge to an entirely different solution [14]. Also, this algorithm needs derivative during the optimization process, which may be difficult to calculate. Bounekhla, Zaim, and Rezzoug [15] proved the Rosenbrock method is better than scatter search and Hook and Jeeves methods in terms of fast and efficient search. Apart from conventional methods, some of the evolutionary techniques like genetic algorithm (GA) [16], genetic programming [17], particle swarm optimization (PSO) [18], differential evolution (DE) [19] evolution strategy [20] and a PSO variant [20] have been successfully

applied to induction motor parameter (electrical and mechanical) estimation. In the present study, PSO is used in situ efficiency determination of induction motor.

Losses in induction motor:

The efficiency can be defined from the individual loss terms as:

$$\eta = \frac{P_{out}}{P_{in}} = \frac{(P_{in} - P_{loss})}{P_{in}} = 1 - \frac{P_{loss}}{P_{in}} \quad 5.1$$

Therefore in principle three types of efficiency measurements may be used:

- Direct measurement of electrical input and mechanical output power
- Direct measurement of the overall losses and the input power
- Measurement of the individual loss components and the input power

The measurement of input power is required in all three methods. Generally, electric power can be measured very accurately, as power meters with accuracy of class 0.2 have been available since the very early stages of alternating current technique. However, the assessment of the mechanical power was more difficult. Nowadays it is possible to measure torque and speed sufficiently accurate in order to obtain correct efficiency values, as shown further on. The measurement of the overall losses is based on calorimetric techniques. Such measurements are very difficult to perform and the accuracy obtained is comparable to the one found by the direct measurement of the output power. The individual loss components are the following:

$$P_{loss} = P_{J1} + P_{J2} + P_{mech} + P_{iron} + P_{addition} \quad 5.2$$

Where,

- P_{J1} : Stator joule losses obtained from the measurement of the stator resistance corrected for temperature
- P_{J2} : Rotor joule losses obtained from the slip corrected for temperature
- P_{iron} : Iron losses, mostly situated in the stator iron, obtained from a no-load test
- P_{mech} : Mechanical friction and windage losses, obtained from the no-load test at different voltages
- $P_{additional}$: Additional load losses i.e. losses not covered by the other loss components, also referred to as stray load losses or supplementary losses.

The first four power loss components are not much debated. The last component, the additional load losses, has been identified as critical component, which determines the variation of efficiency among the standards.

5.2 Standards for induction motor efficiency determination:

The methods for efficiency measurements can roughly be divided into two categories: direct and indirect methods [16]. The main difference between them is that in the direct methods the torque has to be assessed in one way or another. Three different standards are discussed: IEEE standard 112, IEC standard 34-2 and JEC standard. JEC standard totally neglects the stray load losses and always shows a higher efficiency than when tested using IEEE or IEC.

5.2.1 IEEE method 112-1996:

The IEEE 112-1996 consists of five basic methods to determine the efficiency: A, B, C, E and F [16]. In method A, the input and output power is measured and the efficiency is directly obtained as the ratio of output power to input power. This method is only used for very small machines. Method B employs a direct method to obtain the stray load losses. It is not a direct method for determining the motor efficiency. To reduce the influence of the measuring error, a linear regression is made of the stray load losses at different loads, versus the torque squared. Method B is the recommended method for testing of induction machines up to 180 kW.

Method C is a back to back machine test. The total stray load losses are also obtained via a separation of losses for both motor and generator. The stray load losses are then divided between the motor and generator proportional to the rotor currents. Method E and method E₁ are indirect methods; the output power is not measured. In method E the stray load losses are directly measured using the reverse rotation test. In method E₁, the stray load losses are set to an assumed value. For a 3.74 KW induction motor, stray load losses are assumed to be 1.8% of output power.

In method F and F₁, the equivalent circuit of the machine is used. The stray load losses are again directly measured or in the case of F₁ an assumed value is used. There also exist some additional methods as the use of the equivalent circuit but calibrated at a load point. Motors with ratings higher than 180 kW can be tested using methods B, C, E, E₁, F or F₁.

5.2.2 IEC 34-2 method:

For poly phase induction machines, the preferred method of determining efficiency is the summation-of-losses method. Because of the unavoidable measurement errors, direct determination by measuring the power input and output is generally not accurate enough at efficiency >90% and is therefore usually applied only in the range <100 kW [21].

According to the summation-of-losses method, efficiency is determined by calculating total losses without concentrating on output power. The total losses are as follows,

(1) Losses assumed to be constant

(a) Losses in active iron (hysteresis and eddy-current losses including additional No- load stray losses)

(b) Friction losses

(c) Windage losses

(2) Current (load)-dependent losses

(a) I^2R losses in the stator winding

These losses are calculated from the winding resistances and from the current corresponding to the load considered. The resistance values are determined on the basis of a reference temperature specified as a function of the temperature class of the insulation system (for example 75°C for class B).

(b) I^2R losses in the rotor winding

These losses are derived from an on-load test and are taken to be equal to the product of the slip and the total power transmitted to the rotor.

(3) Additional load losses

(a) additional losses occurring at load in active iron and other metal parts

(b) eddy-current losses in the stator and rotor windings caused by current-dependent leakage fields.

In accordance with IEC 34-2, these additional load losses are assumed to be equal to an estimated 0.5% of the power input P_i and to vary as the square of the stator current [16].

5.2.3 JEC method:

This standard is less restrictive of the USA and European standards. The efficiency evaluation through the Japanese standard can be considered as an indirect method. This method neglects the stray losses [22]. For these reason, the obtained efficiency values are generally

higher. Furthermore, no thermal correction of the Joule losses is specified because it is very difficult to find the measurement procedures prescribed by the Japanese standard, it is reasonable to evaluate the machine efficiency using the results of the test which are required by the other Standards [22].

5.3 Optimization algorithm used:

Standard Particle Swarm Optimization:

The concept of PSO was first suggested by Kennedy and Eberhart in 1995 [23]. The mechanism of PSO is inspired from the complex social behaviour shown by the natural species. For a D-dimensional search space the position of the i^{th} particle is represented as

$X_i = (x_{i1}, x_{i2}, \dots, x_{iD})$. Each particle maintains a memory of its previous best position

$P_{\text{best } i} = (p_{i1}, p_{i2}, \dots, p_{iD})$. The best one among all the particles in the population is represented as $P_{\text{gbest}} = (p_{g1}, p_{g2}, \dots, p_{gD})$. The velocity of each particle is represented as

$V_i = (v_{i1}, v_{i2}, \dots, v_{iD})$. In each iteration, the P vector of the particle with best fitness in the local neighbourhood, designated g, and the P vector of the current particle are combined to adjust the velocity along each dimension and a new position of the particle is determined using that velocity [21]. The two basic equations that govern the working of standard PSO (SPSO) are that of velocity vector and position vector given by

$$v_{id} = wv_{id} + c_1r_1(p_{id} - x_{id}) + c_2r_2(p_{gd} - x_{gd}) \quad 5.3$$

$$x_{id} = x_{id} + v_{id} \quad 5.4$$

The first part of Eq. (5.3) represents the inertia of the previous velocity, the second part is the cognition part that tells us about the personal experience of the particle and the third part represents the cooperation among particles and is named as the social component. Acceleration constants c_1 , c_2 and inertia weight w are predefined by the user and r_1 , r_2 are the uniformly generated random numbers in the range of [0, 1].

5.4 In-situ Efficiency determination:

The general block diagram of in situ efficiency determination of induction motor using optimization algorithms is shown in Fig.5.1 [24].

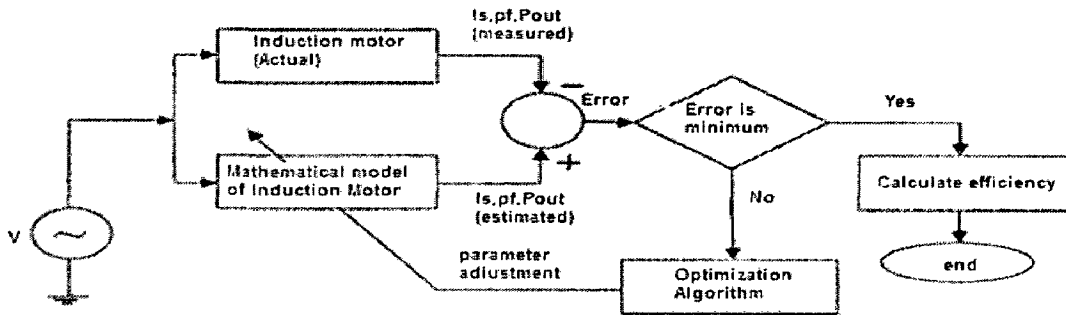


Fig.5.1 Block diagram of induction motor in-situ efficiency determination.

First, the stator line resistance is measured after shutting down the motor. 5hp, four-pole induction motor considered as test motor. “Summation of losses” method for efficiency determination is used with the assumption of stray load losses. The winding arrangement of a star connected motor is shown in Fig.5.2 and the resistance per phase is calculated as in Eq. (5.5).

$$r_1 = \frac{r_{1line}}{2} \tag{5.5}$$

Where r_{1line} is stator line resistance and r_1 is stator phase resistance.

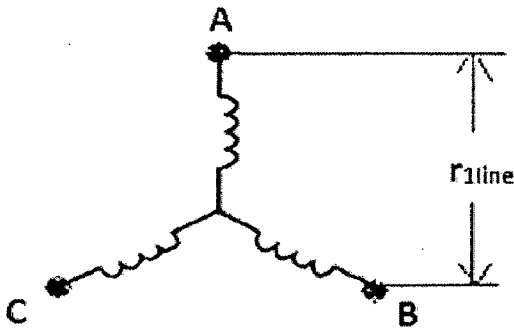


Fig.5.2 Winding arrangement of star connected motor

Some measurements on the motor are required before running the optimization algorithm to estimate the motor parameters: stator line to line voltage V_1 , stator current I_1 , input power P_{inp} and rpm at difference load points [24]. Then, power factor can be calculated as in Eq. (5.6). The measured and calculated values of the test motor for a wide range of loads and the equivalent circuit considered here is taken from Pillay et al. [25] and is shown in Fig.5.3.

$$pf = \frac{P_{inp}}{\sqrt{3}V_1I_1} \tag{5.6}$$

The recommended value of stray load losses for different capacity motors is shown in Table 5.1 (IEEE standard 2004). In the present study we considered this loss at full load is 1.8% and its calculation at different load point is shown in Eq. (5.7).

Table 5.1 Stray Load Losses for the Different Capacity Motors (IEEE standard 2004)

Motor rated power	Stray load loss relative to output power(%)
0.75-90 kW	1.8
91-375 kW	1.5
376-1800 kW	1.2
1800 kW and higher	0.9

$$P_{st} = P_{stfl} \frac{I_2^2}{I_{2fl}^2} \tag{5.7}$$

Where P_{st} , P_{stfl} are stray load losses at any point and full load respectively and I_2 , I_{2fl} are rotor currents at these load points.

The stray load loss resistance r_{st} is

$$r_{st} = 0.018r_2 \frac{(1-s_{fl})}{s_{fl}} \tag{5.8}$$

Temperatures of stator and rotor windings are assumed to be the same and calculated as in Eq. (5.9) with the IEEE recommended reference temperature.

$$T_t = \frac{I_1 - I_0}{I_{fl} - I_0} (T_r - T_s) + T_s \tag{5.9}$$

Where I_1 , I_{fl} are the measured and nameplate stator currents, I_0 is the stator current under no-load DC test, $T_r=75^\circ\text{C}$ is the reference temperature for the insulation system of class A (IEEE standard 2004) and $T_s=25^\circ\text{C}$ is the ambient temperature.

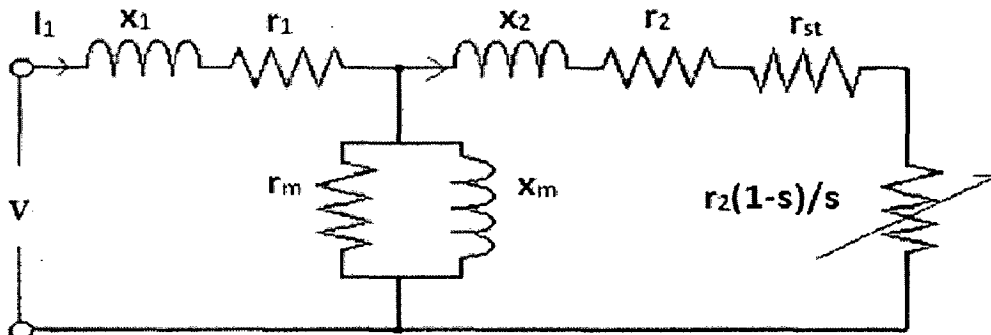


Fig.5.3 Equivalent circuit of induction motor with stray loss resistance

The stator and rotor resistances are corrected to the test temperature as:

$$r_{1c} = \frac{r_1(T_t + k_c)}{(T_s + k_c)} \quad 5.10$$

$$r_{2c} = \frac{r_2(T_t + k_a)}{(T_s + k_a)} \quad 5.11$$

Where r_1 is the stator resistance measured during DC test and r_2 is the assumed rotor resistance. The complex admittances of the branches of the equivalent circuit of Fig.5.3 are given below [25].

$$\bar{Y}_2 = \frac{1}{\frac{r_{2c}}{s} + r_{st} + jx_2} \quad 5.12$$

$$\bar{Y}_m = \frac{-j}{x_m} + \frac{1}{r_m} \quad 5.13$$

The stator current can be estimated as

$$I_{1est} = |\bar{I}_1| = \left| \frac{\bar{V}_1 \bar{Y}_1 (\bar{Y}_2 + \bar{Y}_m)}{\bar{Y}_1 + \bar{Y}_2 + \bar{Y}_m} \right| \quad 5.14$$

Where,

$$\bar{V}_1 = \frac{V_1}{\sqrt{3}}$$

The power factor and rotor current can be estimated as

$$pf_{est} = \frac{\Re(\bar{I}_1)}{I_{1est}} ; I_2 = \left| \frac{\bar{V}_1 \bar{Y}_1 \bar{Y}_2}{\bar{Y}_1 + \bar{Y}_2 + \bar{Y}_m} \right| \quad 5.15$$

The current through r_m for the circuit of Fig.5.3:

$$I_m = \left| \frac{\bar{V}_1 \bar{Y}_1}{r_m (\bar{Y}_1 + \bar{Y}_2 + \bar{Y}_m)} \right| \quad 5.16$$

The input power of the circuit of Fig.5.3 can be estimated as

$$P_{inpest} = 3(I_1^2 r_{1c} + I_2^2 (r_{2c}/s + r_{st}) + I_m^2 r_m) \quad 5.17$$

The output power can be estimated as

$$P_{outest} = 3I_2^2 r_{2c} \frac{1-s}{s} \quad 5.18$$

The efficiency can be estimated as

$$\eta = \frac{P_{outest}}{P_{inpest}} * 100\% \quad 5.19$$

The goal of the PSO is to minimize the errors between the measured and calculated parameters. In the present study, two methods of objective functions are considered and are taken from [24].

In method 1, input power and stator current are considered and the objective function to be maximized is:

$$Maxff_1 = \frac{1}{f_1^2 + f_2^2} \quad 5.20$$

Where $f_1 = (I_{1est} - I_1) \frac{100}{I_1}$ and $f_2 = (P_{inest} - P_{in}) \frac{100}{P_{in}}$

In method 2, input power, stator current and power factor are considered and the objective function to be maximized is:

$$Maxff_2 = \frac{1}{f_1^2 + f_2^2 + f_3^2} \quad 5.21$$

Where f_1, f_2 are same as in objection function ff_1 and $f_3 = (pf_{est} - pf) \frac{100}{pf}$.

The decision variables of the above objective functions are x_1, r_2, x_m and r_m . Optimization algorithm is used to determine the above said unknown variables.

5.5 Experimental Setup and Parameter Settings:

5.5.1 Experimental setup:

The experimental setup for testing 3.74 kW induction machine is shown in Fig.5.4. The machine is loaded by a DC motor equipped with a four quadrant rectifier feeding the energy back to the supply. The input power, input voltages and currents are measured using voltage and non-contacting current probes. Although the measurement data are the same, the efficiency at different standards differs substantially due to different additional losses accounted by each method.

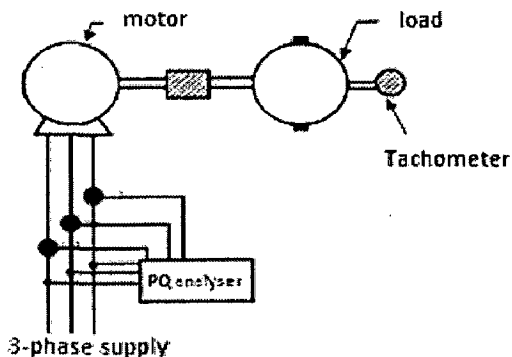


Fig.5.4 Experimental setup for determining induction motor efficiency

5.5.2 Parameter settings:

For the PSO algorithm the inertial weight w is taken to be linearly decreasing from 0.9 to 0.4 and the acceleration constants c_1 and c_2 are taken as 1.49 each. The assigned parameters of the given motor are $K_a=225$, $K_c=234.5$, $r_1=4.69$ ohm, I_0 (No-load current) = 1.9 A, poles=4, supply frequency=50 Hz.

Table 5.2 Voltage, current, power input, speed and power factor at various load points

Load Points	Voltage input(V)	Power input(W)	Line current(A)	Actual speed(rpm)	Power factor
1	425	1460	3.4	1432	0.58
2	425	2100	4	1428	0.7
3	425	3090	5.4	1402	0.8
4	425	3900	6.5	1392	0.84

Table 5.3 Efficiency calculation of induction motor by IEEE

Load Points	Constant loss(W)	Slip	St Cu Loss(W)	Ro Cu Loss(W)	Stray loss(W)	Power Out(W)	Efficiency (%)
1	223	0.0202	54.216	23.954	20.859	1137.971	77.943
2	223	0.0162	75.040	29.096	31.912	1740.953	82.902
3	223	0.0408	136.760	111.332	47.140	2571.768	83.229
4	223	0.0476	198.152	165.659	59.637	3253.551	83.424

Table 5.4 Efficiency calculation of induction motor by IEC

Load Points	Costant loss(W)	Slip	St Cu Loss (W)	Ro Cu Loss (W)	Addl loss (W)	Power Out(W)	Efficiency (%)
1	223	0.0202	54.216	23.954	7.3	1151.53	78.872
2	223	0.0229	75.040	29.096	10.5	1762.364	83.922
3	223	0.0408	136.760	111.332	15.45	2603.458	84.254
4	223	0.0476	198.152	165.659	19.5	3293.688	84.454

Table 5.5 Efficiency calculation of induction motor by JEC

Load Points	Constant loss(W)	Slip	St Cu Loss(W)	Ro Cu Loss(W)	Power Out(W)	Efficiency (%)
1	223	0.0202	54.216	23.954	1158.83	79.372
2	223	0.0229	75.040	29.096	1772.864	84.422
3	223	0.0408	136.760	111.331	2618.908	84.754
4	223	0.0476	198.152	165.659	3313.188	84.954

Table 5.6 Error calculation for different standards using objective functions ff_1 , ff_2

Load Point	Estimated Eff. (%)		Error w.r.t. ff_1			Error w.r.t. ff_2		
	ff_1	ff_2	IEEE	IEC	JEC	IEEE	IEC	JEC
1	81.957	81.625	4.014	3.085	2.585	3.682	2.753	2.253
2	81.579	81.377	-1.323	-2.343	-2.843	-1.525	-2.545	-3.045
3	77.207	77.306	-6.022	-7.047	-7.547	-5.923	-6.948	-7.448
4	74.513	74.678	-8.911	-9.941	-10.441	-8.746	-9.776	-10.276

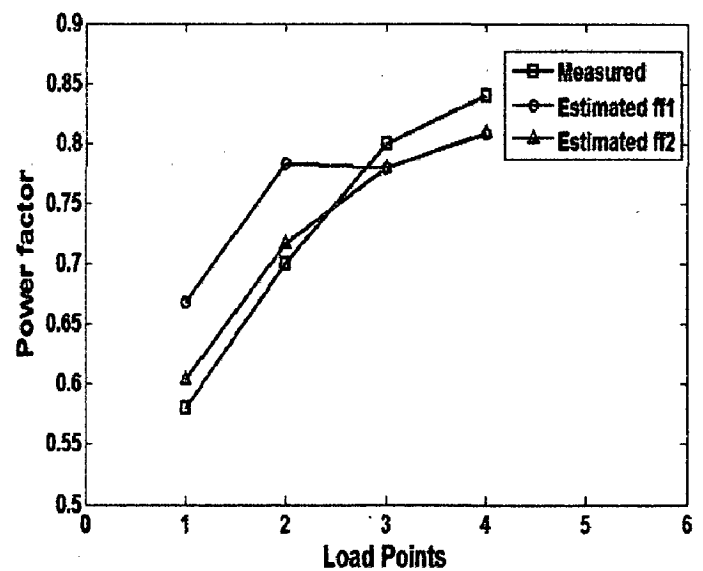
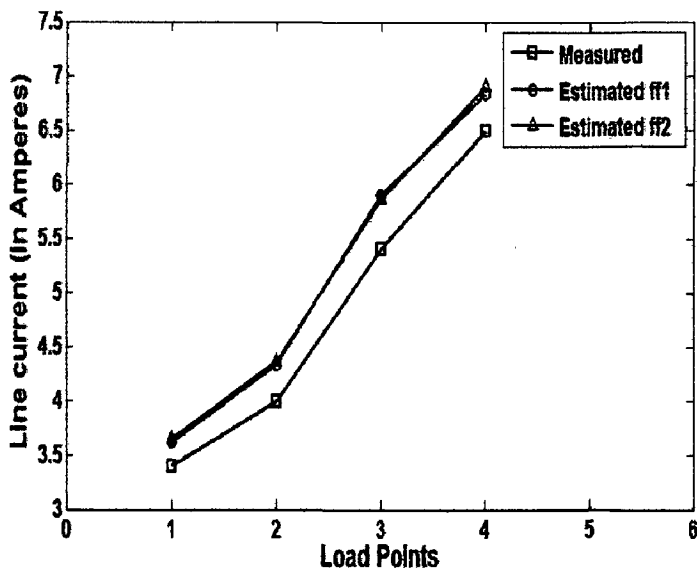


Fig.5.5 Comparison of measured and estimated (i) line currents and (ii) power factor of 3.74 KW induction motor respectively

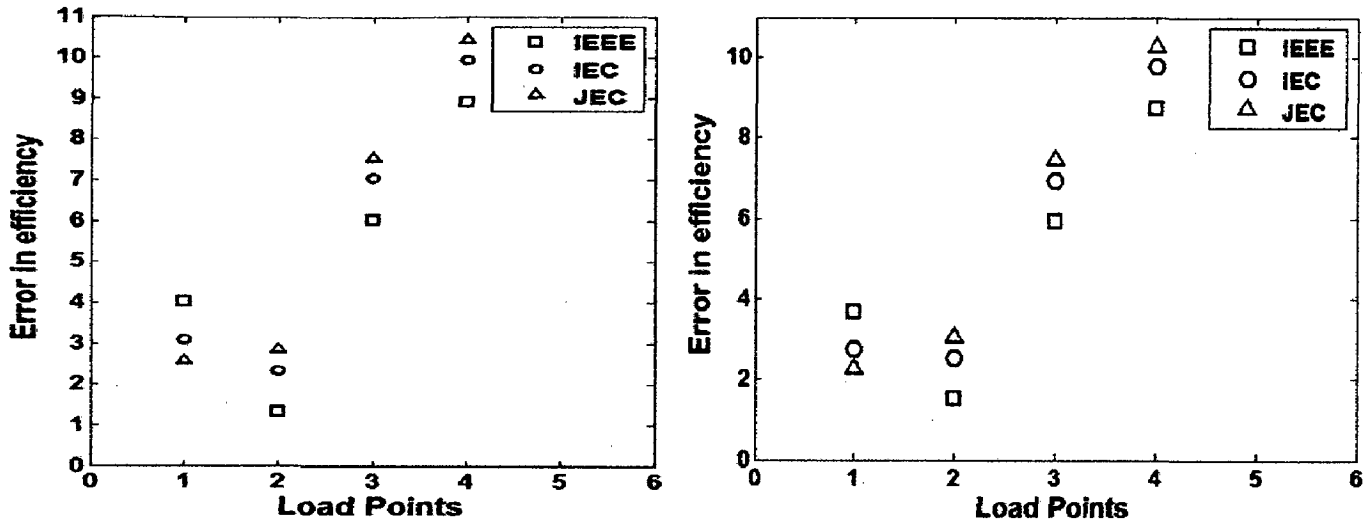


Fig.5.6 Comparison of error in efficiency for different standards and at different load points for objective function (i) ff_1 and (ii) ff_2 .

5.6 Results and Discussion:

The efficiency calculation for different standards namely IEEE, IEC and JEC are shown in Tables 5.3 to 5.5. Table 5.6 shows the error calculation for different standards using objective functions ff_1 and ff_2 . Fig.5.5(i) and Fig.5.5(ii) give a comparison of measured and estimated line currents and power factor respectively. Fig.5.6 (i) shows variation of error in efficiency with load for different standards using objective function ff_1 . From the results, it can be observed that at load point 1, minimum error is obtained using JEC standard. Similarly, at load point 2, 3 and 4 minimum error is obtained using IEEE standard. Similar trend is followed in case of objective functions ff_2 shown in Fig.5.6(ii) i.e. at load point 1, error is minimum for JEC and at load points 2, 3 and 4 error is minimum for IEEE. From Table 5.6, it can be seen that for all the three standards, error is minimum in case of ff_2 . So, only three input parameters namely stator current, input power and power factor are sufficient to determine the motor parameters quickly.

5.7 Conclusion:

In this paper, particle swarm optimization is used for in-situ efficiency determination of induction motor (5 hp) without performing no-load test. Results are compared with actual values. The error between estimated and actual efficiencies is found for different methods. The differences in methods were based on the number of input parameters used in the optimization algorithm. In-situ efficiency of induction motor can be accurately calculated by using input power, current and power factor as the input parameters of optimization algorithm. Also, IEEE standard leads to minimum error compared to other standards, namely IEC and JEC.

Simulation Results and Discussions

[This chapter deals with MATLAB simulations regarding energy efficient control of induction motor drive through loss model control and sensitivity analysis of loss model controller under parameter variation.]

6.1 Introduction:

The proposed work involves closed loop vector controlled induction motor drive with LMC for efficiency control. The detailed analysis and the results obtained when energy controller i.e. LMC is used are compared with constant flux operation when no LMC is used.

Parameters of the motor, for simulation are given in Table (6.1).

Table 6.1 Induction Motor Parameters for Simulation

<i>parameter</i>	stator	rotor
Resistance	11.124 ohms	8.9838 ohms
Leakage inductance	0.03336 H	0.03336H
Magnetizing inductance	0.49045 H	
Moment of inertia		0.0018 kg-m ²

For comparison purpose simulation is carried on for same variation in torque and speed. Simulation results are shown in Fig.6.2, 6.3, 6.5, 6.6, 6.8, and 6.9. Three cases are considered here

Case1: Only load torque changes.

Case2: Only speed changes.

Case3: Both load torque and speed change (Mine hoist load diagram in mineral industry).

6.2 Results:

CASE-1: When load changes:

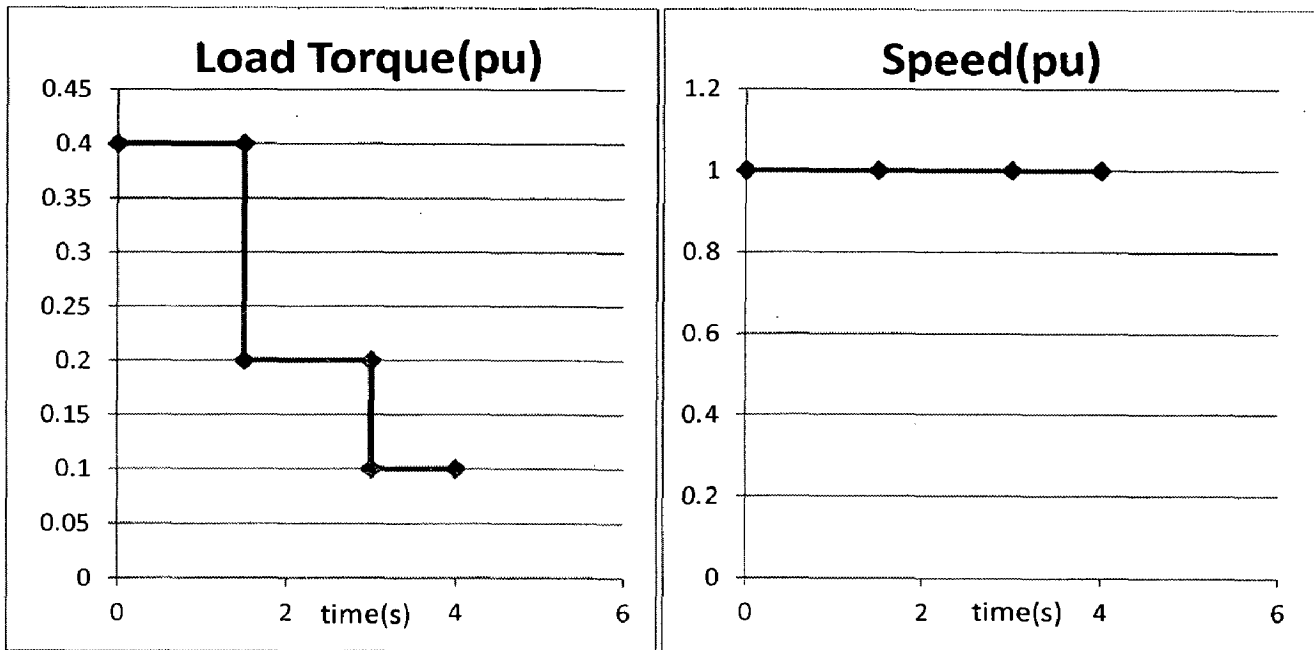


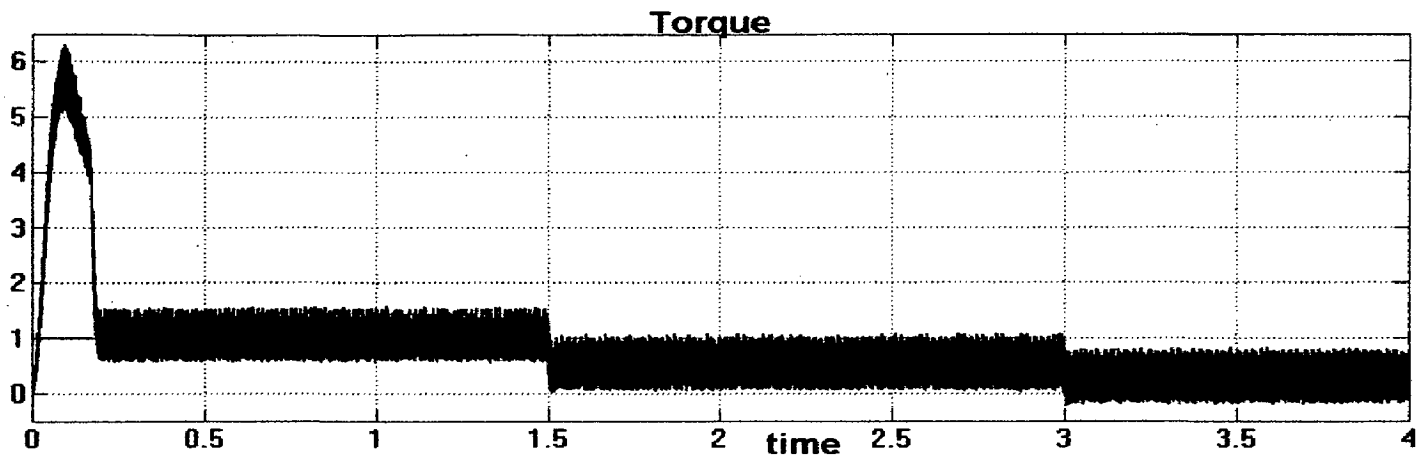
Fig.6.1 Load diagram when only load is changed

Region 1(0-1.5 s): load torque=1.0 Nm (0.4 pu), Speed=300 rad/s (1 pu)

Region 2(1.5-3 s): load torque=0.5 Nm (0.2 pu), Speed=300 rad/s (1 pu)

Region 3(3-4 s): load torque=0.25 Nm (0.1 pu), Speed=300 rad/s (1 pu)

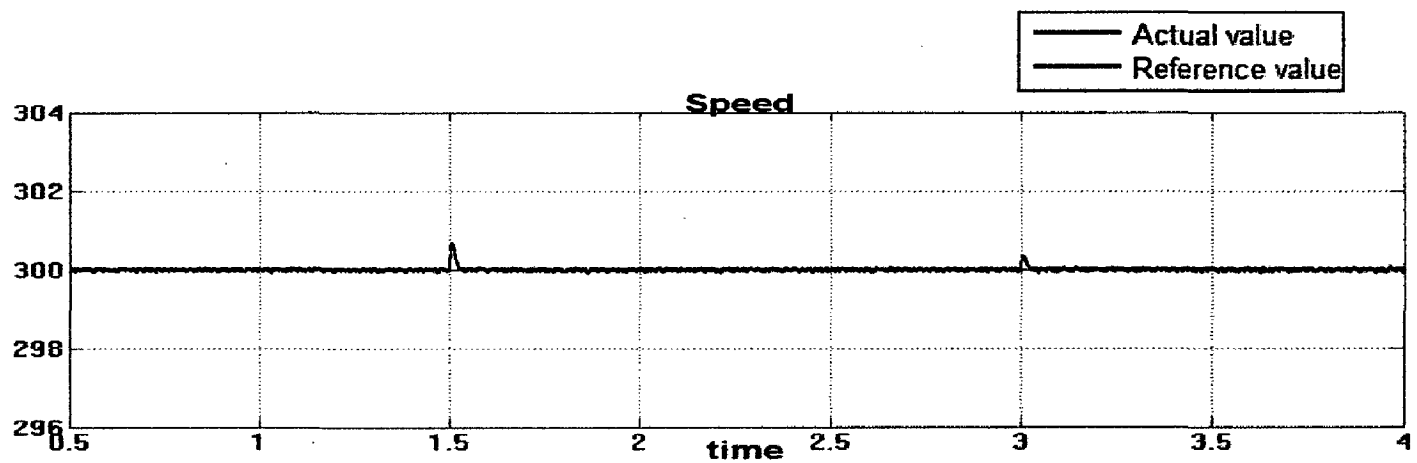
Rated torque = 2.5 Nm, Rated speed = 300 rad/s



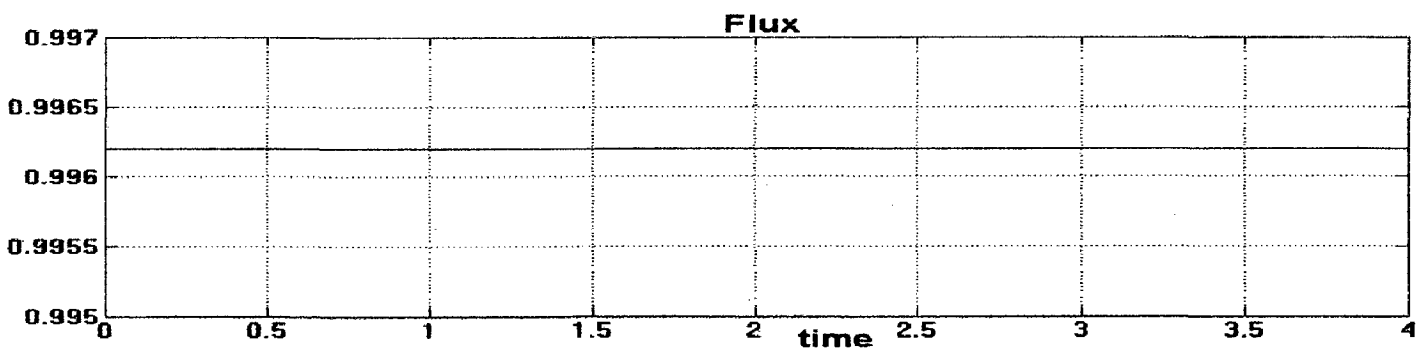
Region 1:
Torque=1 Nm

Region 2:
Torque= 0.5 Nm

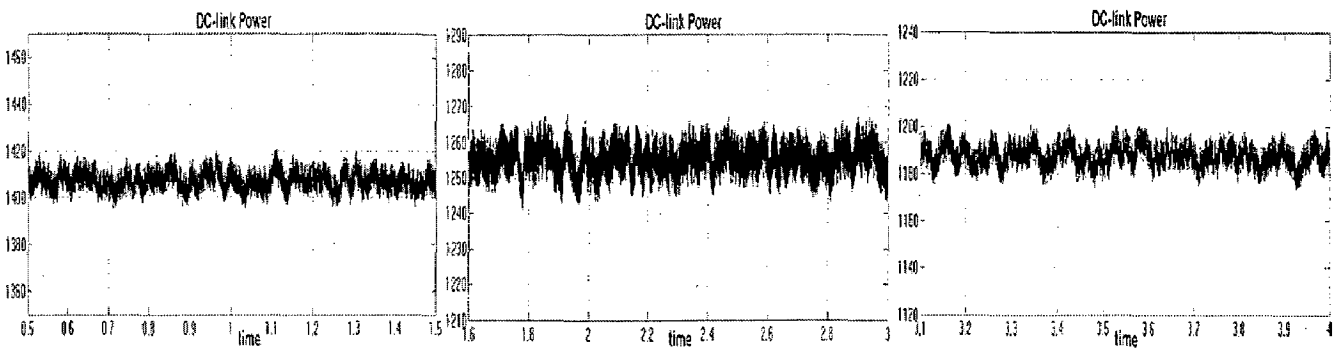
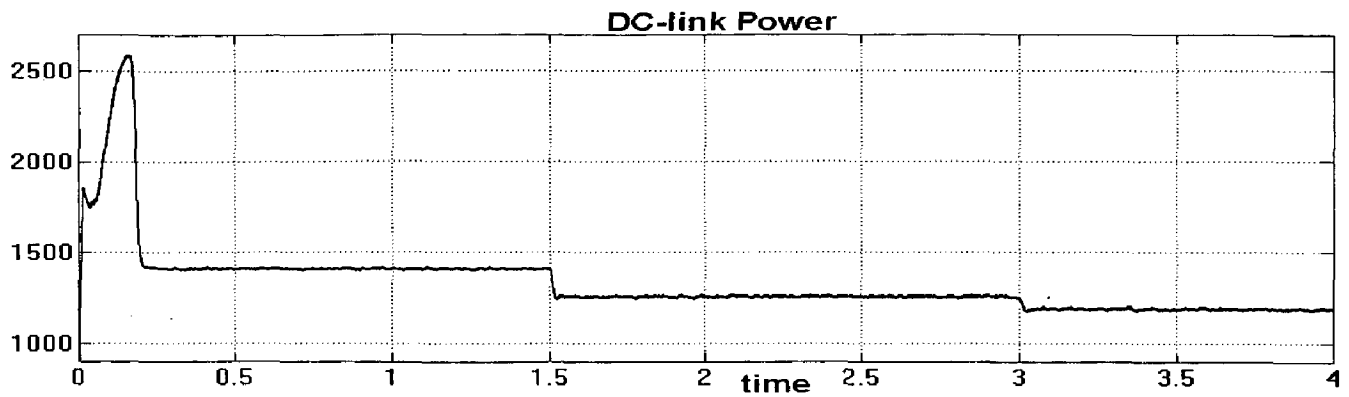
Region 3:
Torque= 0.25 Nm



Speed=300 rad/s



Flux= 0.9962 pu.



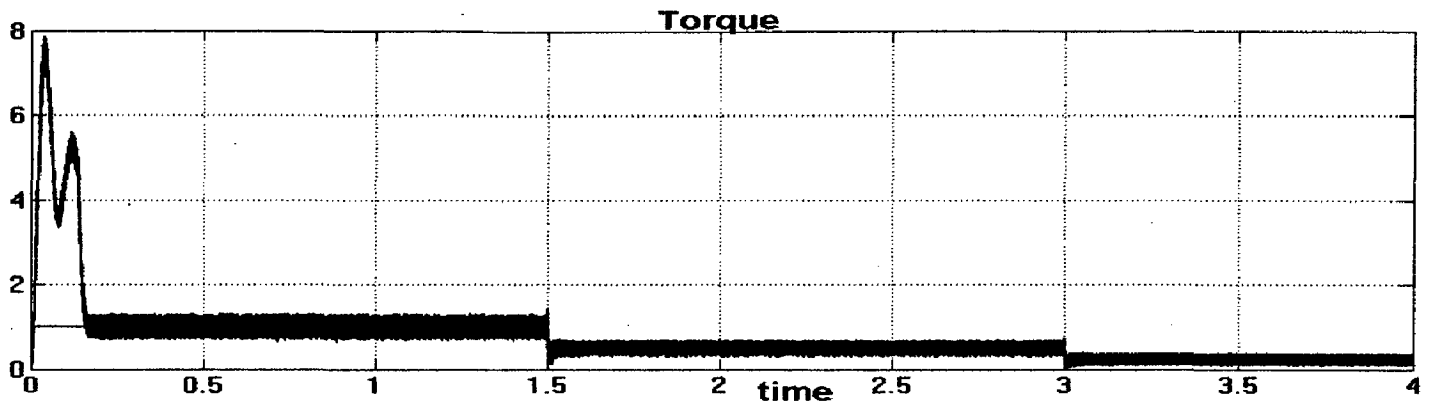
Region 1:
DC-link Power=1410 W

Region 2:
DC-link Power=1255 W

Region 3:
DC-link Power=1190 W

Fig.6.2 Simulation results of vector controlled induction motor drive without loss model control (load changes)

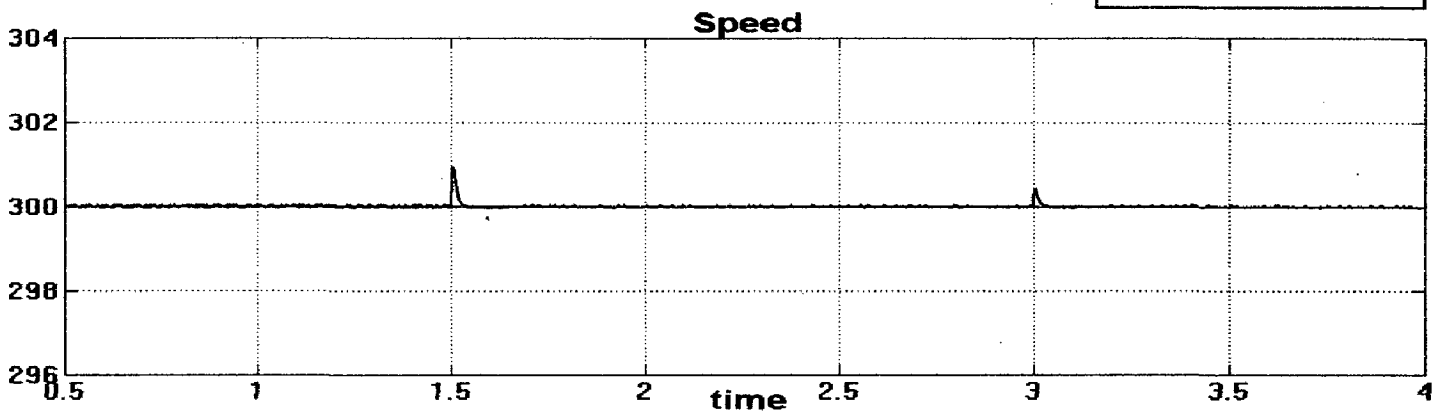
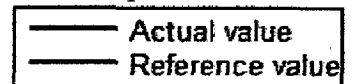
This is the conventional field oriented control (constant flux control) where the flux is always constant (0.9962 pu) irrespective of speed and torque. At light loads, there is no balance between iron and copper losses with more core losses. Hence, efficiency is low. In the present case, speed is kept constant at 300 rad/s and only load is varied. Motor consumes DC-link power of 1410 W in region 1, 1255 W in region 2 and 1190 W in region 3.



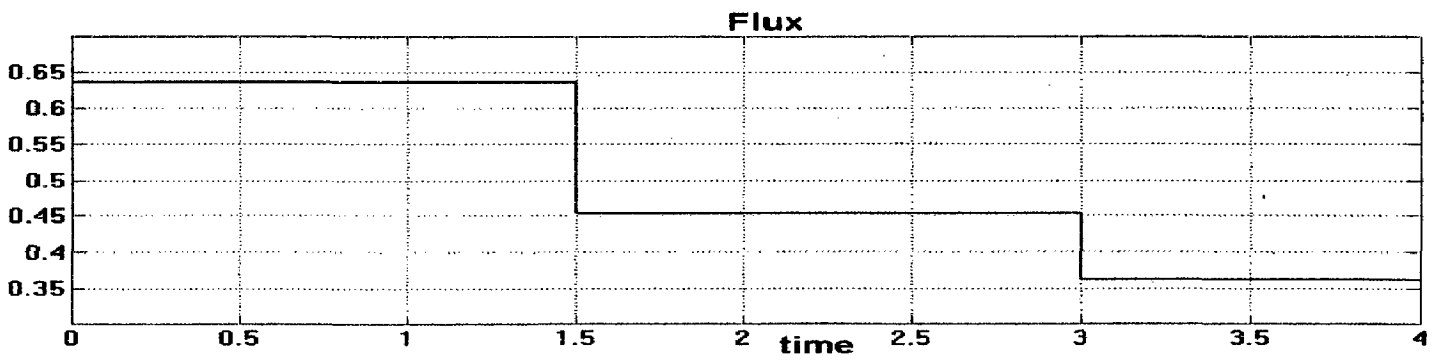
Region 1:
Torque=1 Nm

Region 2:
Torque= 0.5 Nm

Region 3:
Torque= 0.25 Nm



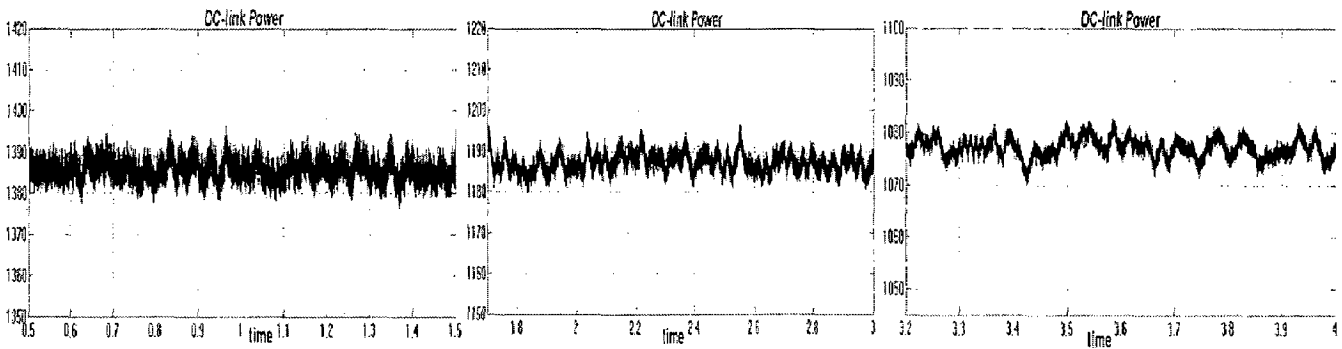
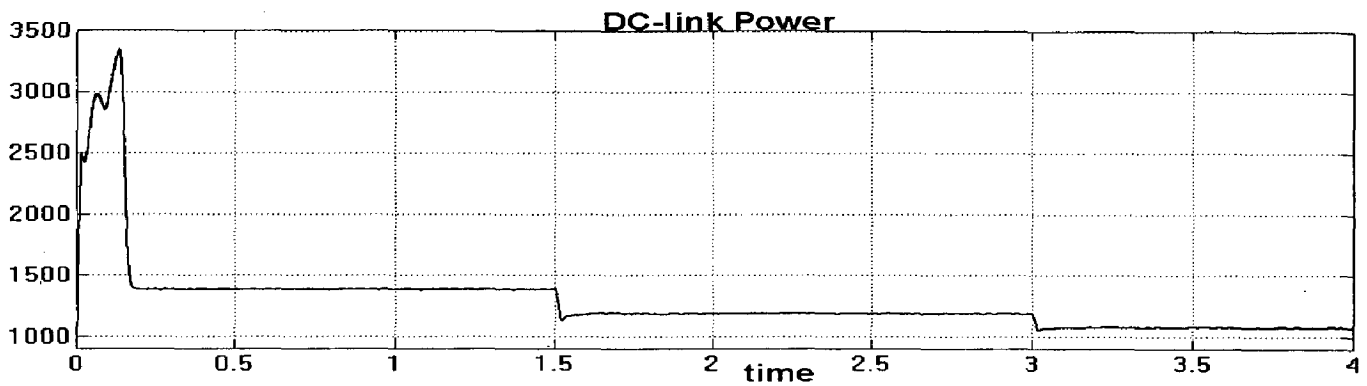
Speed = 300 rad/s



Region 1:
Flux=0.6367 pu

Region 2:
Flux = 0.4532 pu

Region 3:
Flux = 0.3614 pu



Region 1:
DC-link Power=1385 W

Region 2:
DC-link Power=1185 W

Region 3:
DC-link Power=1075 W

Fig.6.3 Simulation results of vector controlled induction motor drive with loss model control (load changes)

Here, optimal value of i_{ds}^* is found from the loss model of the motor in accordance with load and speed. This controller finds optimal i_{ds}^* instantly as shown in Fig.6.3. Since, the adjustment of flux level is mainly required under lightly loaded condition, light loads are considered here. Load torque is varied from 1 Nm in region 1 to 0.5 Nm in region 2. Thus, flux drops from 0.6367 pu to 0.4532 pu. In region 3, load is reduced to 0.25 Nm. Hence, flux being dependent on load decreases to 0.3614 pu. DC link power to the motor with loss model controller is 25 W lesser (saving) than conventional controller in region 1. Similarly, in region 2, DC link power to the motor with LMC is 70 W lesser than conventional controller. In region 3, DC link power to the motor with LMC is 115 W lesser than conventional controller.

CASE-2: When speed changes:

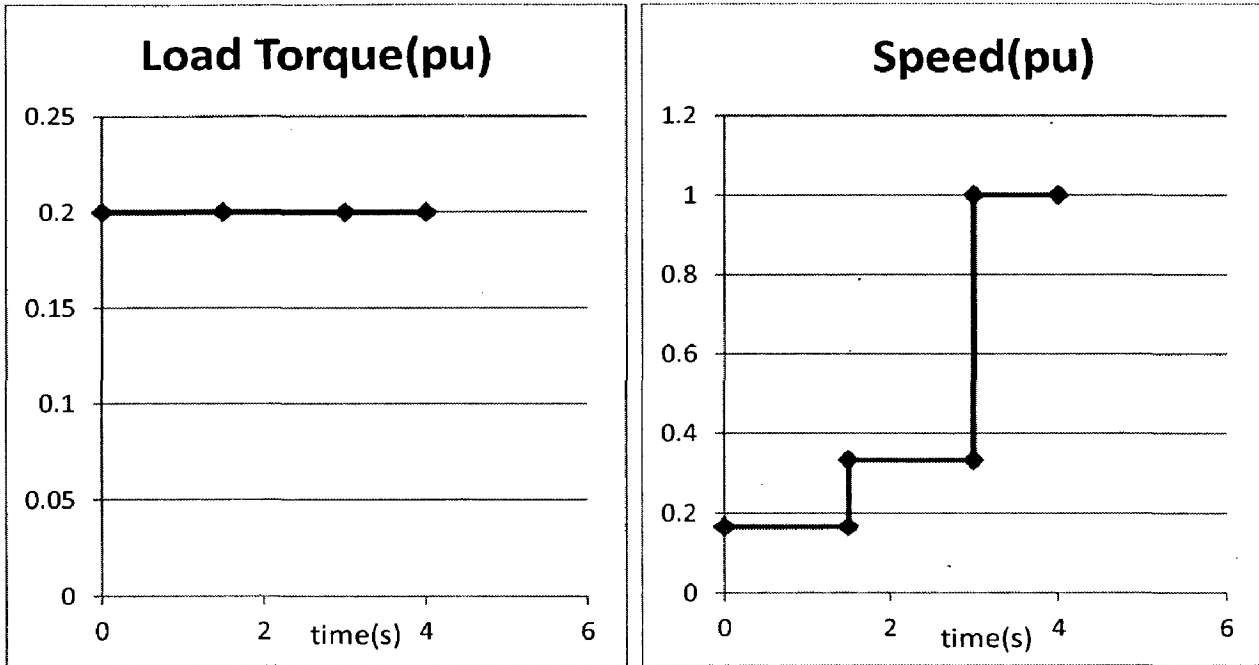
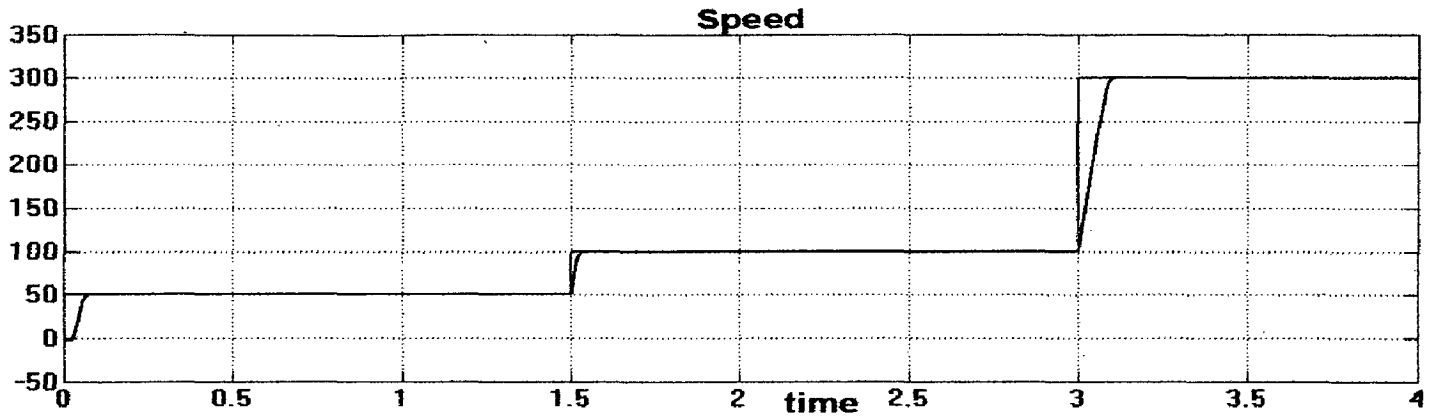


Fig.6.4 Load diagram when only speed is changed

Region 1(0-1.5 s): load torque=0.5 Nm (0.2 pu), Speed=50 rad/s (0.166 pu)

Region 2(1.5-3 s): load torque=0.5 Nm (0.2 pu), Speed=100 rad/s (0.333 pu)

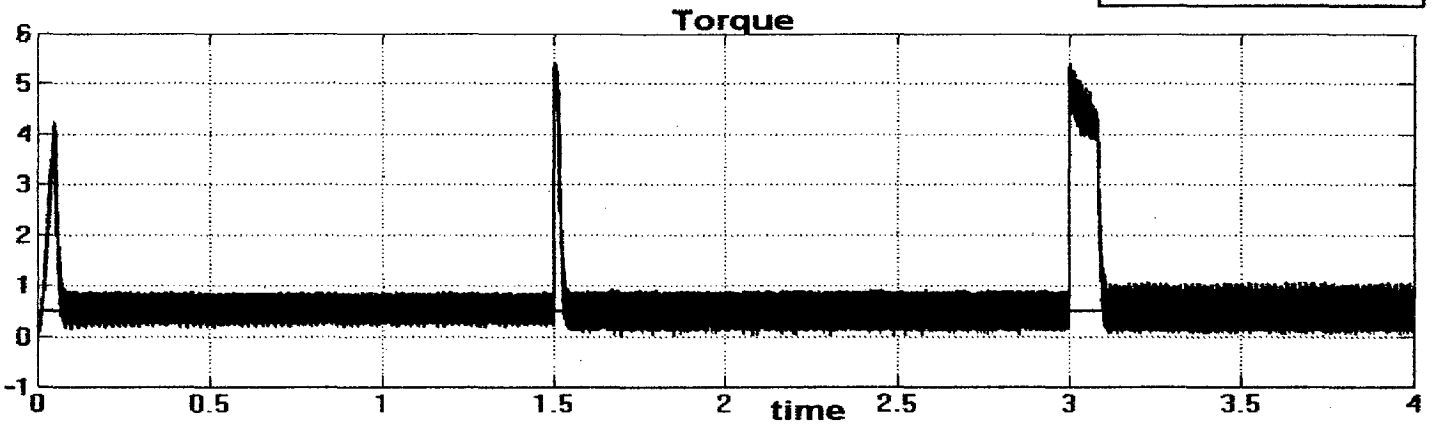
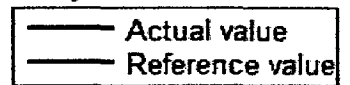
Region 3(3-4 s): load torque=0.5 Nm (0.2 pu), Speed=300 rad/s (1 pu)



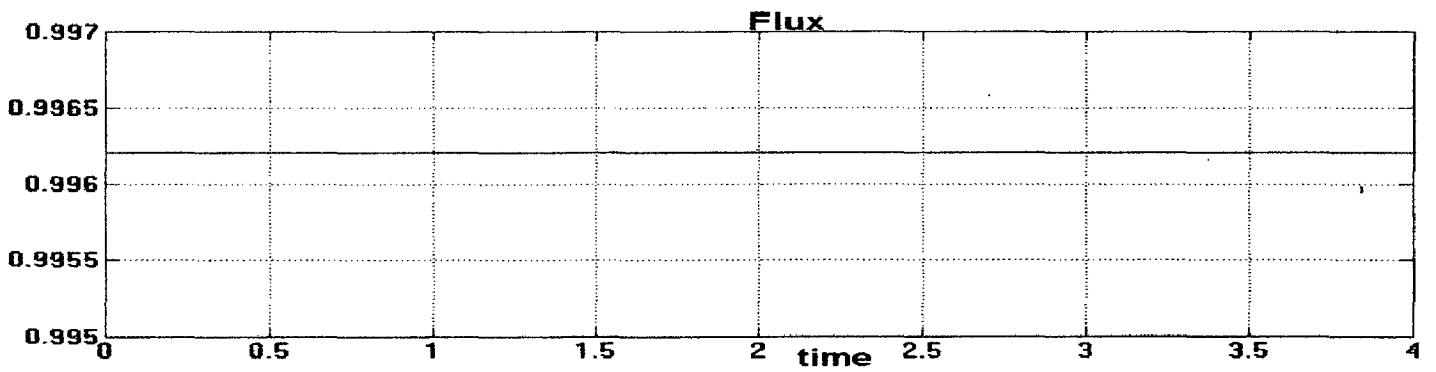
Region 1:
Speed=50 rad/s

Region 2:
Speed = 100 rad/s

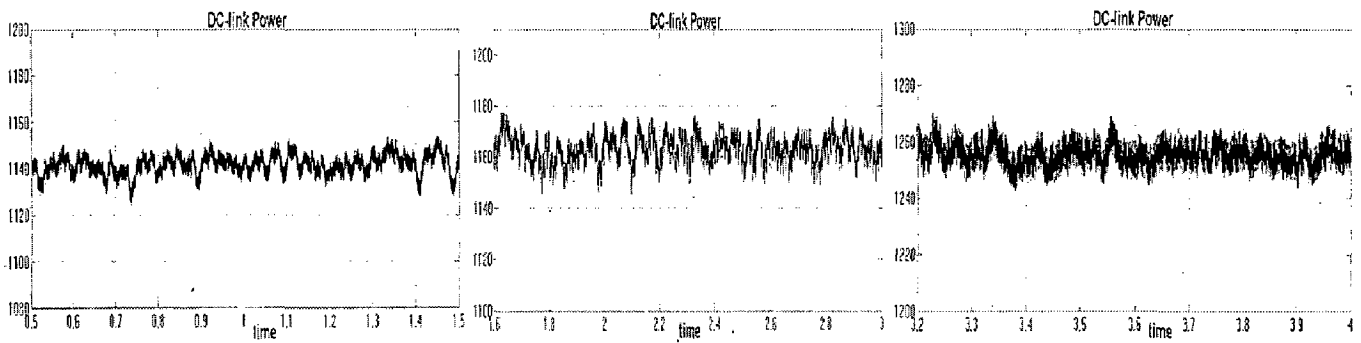
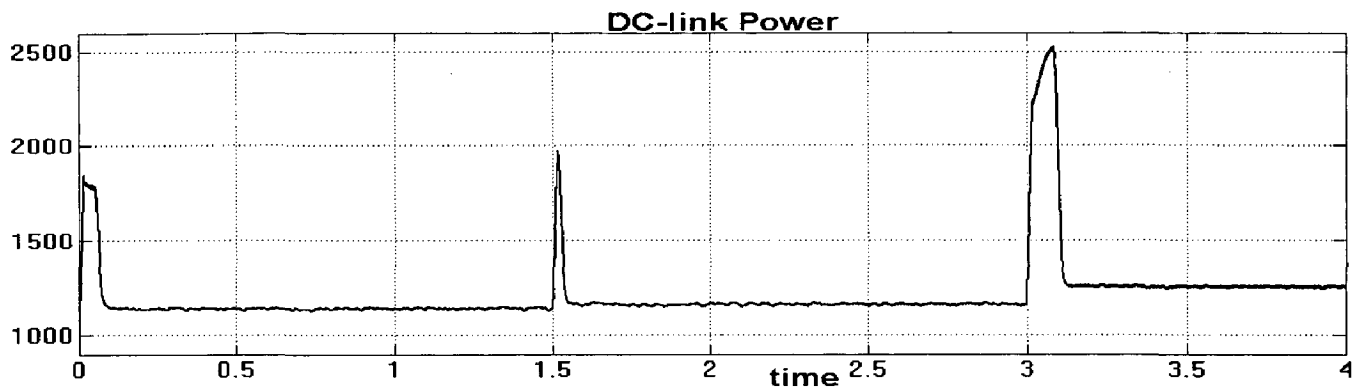
Region 3:
Speed = 300 rad/s



Torque = 0.5 Nm



Flux= 0.9962 pu.



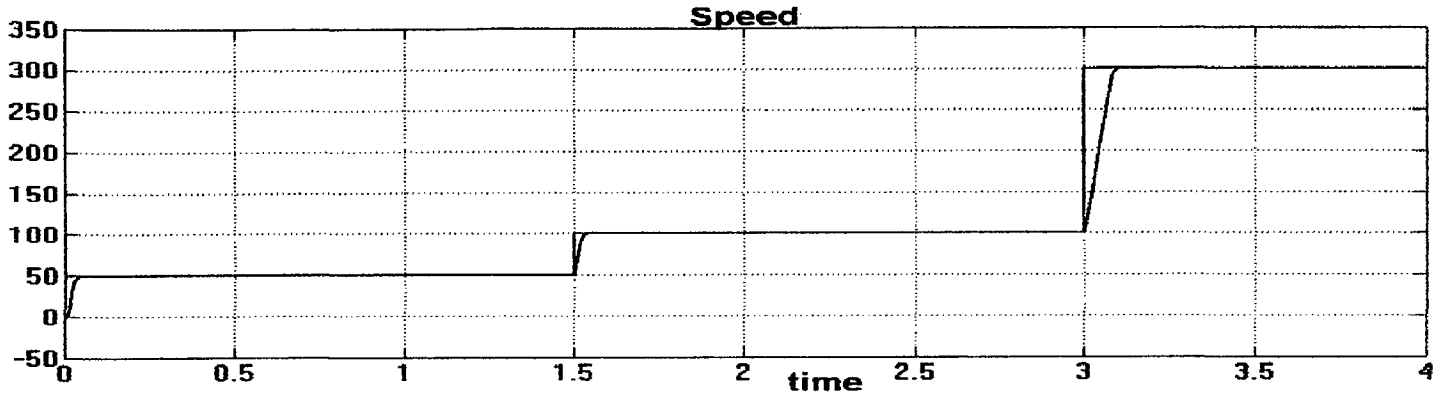
Region 1:
DC-link Power=1140 W

Region 2:
DC-link Power=1160 W

Region 3:
DC-link Power=1255 W

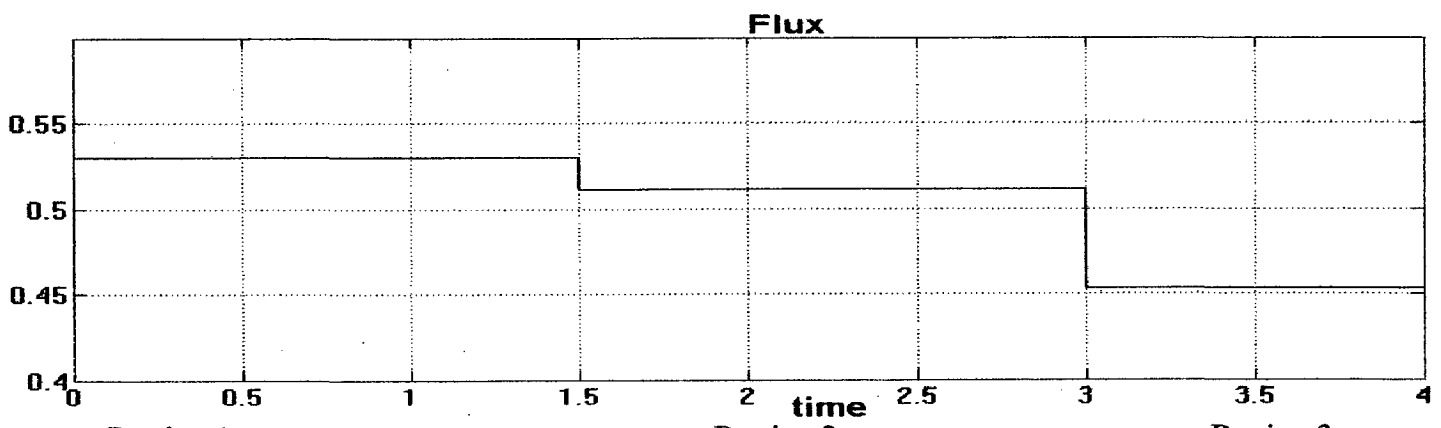
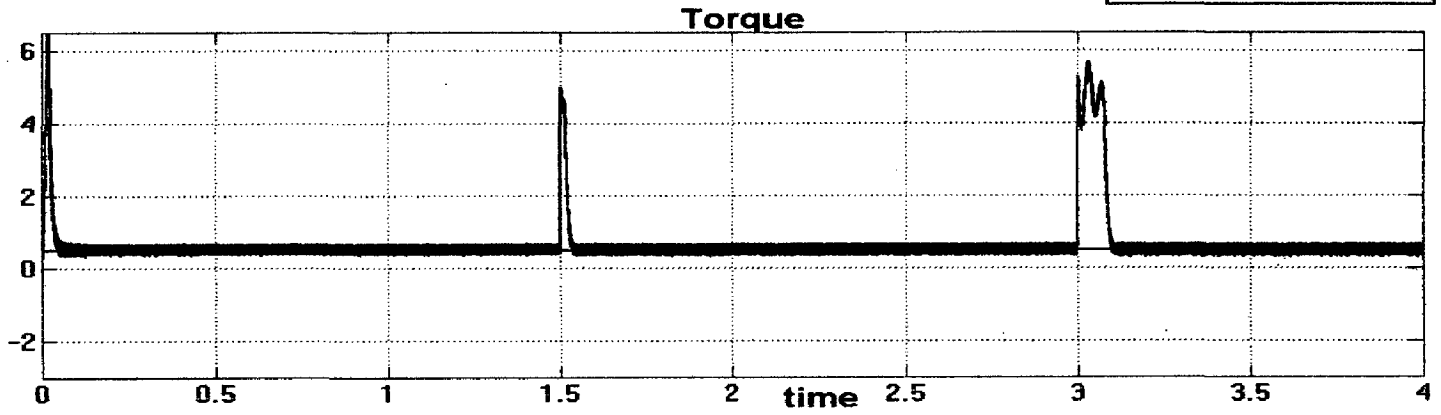
Fig.6.5 Simulation results of vector controlled induction motor drive without loss model control (speed changes)

In this case, load torque is kept constant at 0.5 Nm and only speed is changed. Flux is always constant (0.9962 pu) irrespective of variation in speed. Motor consumes DC-link power of 1140 W in region 1, 1160 W in region 2 and 1255 W in region 3.



Region 1: Speed=50 rad/s Region 2: Speed = 100 rad/s Region 3: Speed = 300 rad/s

— Actual value
 — Reference value



Region 1: Flux=0.5298 pu Region 2: Flux = 0.5113 pu Region 3: Flux = 0.4532 pu

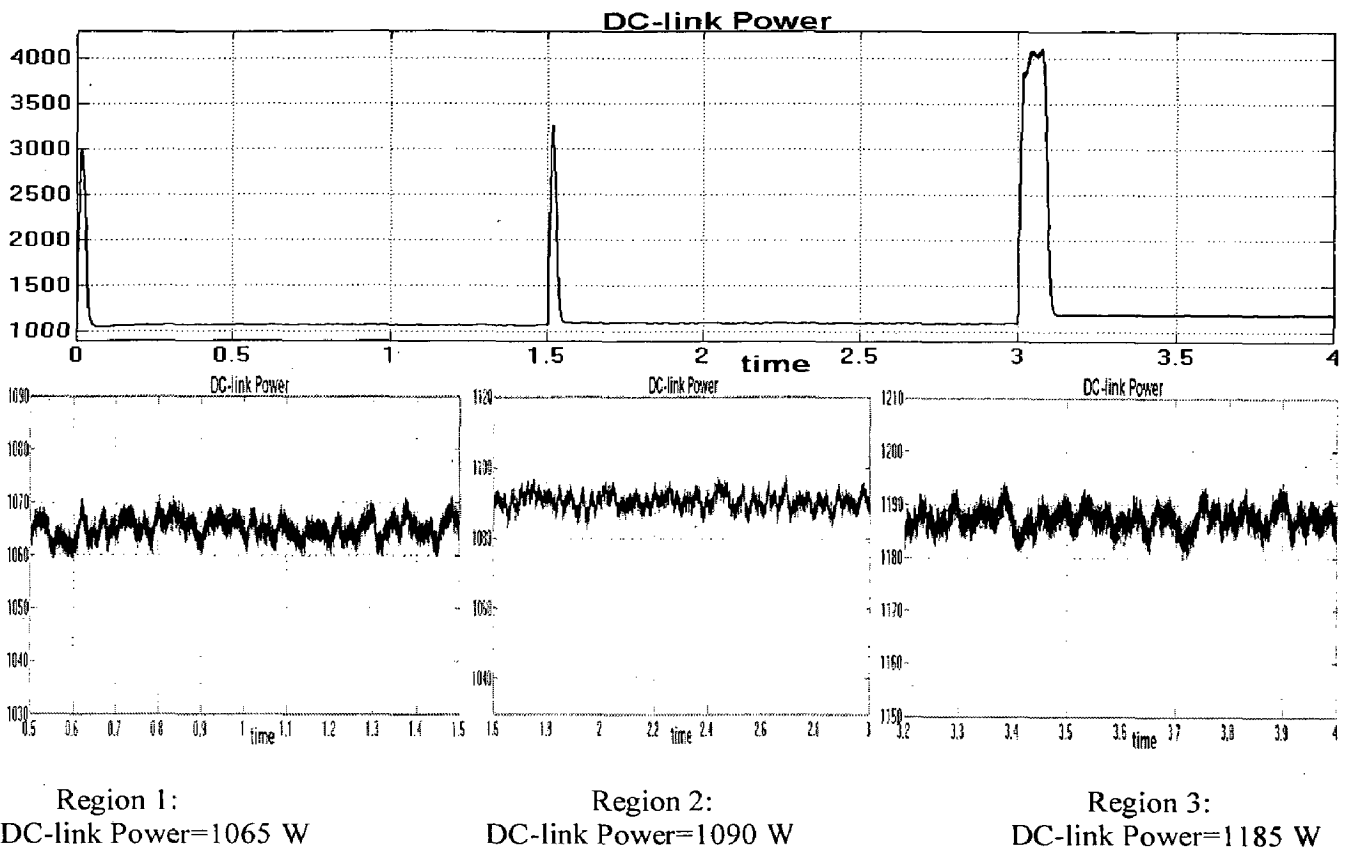


Fig.6.6 Simulation results of vector controlled induction motor drive with loss model control (speed changes)

Since, the adjustment of flux level is mainly required under lightly loaded condition, light load (0.5 pu) is considered here. Speed is varied from 50 rad/s in region 1 to 100 rad/s in region 2. Thus, flux drops from 0.5298 pu to 0.5113 pu. In region 3, speed is increased to 1 pu. Hence, flux being dependent on speed changes to 0.4532 pu. DC link power to the motor with loss model controller is 75 W lesser (saving) than conventional controller in region 1. Similarly, DC link power to the motor with LMC is 70 W lesser than conventional controller in region 2 and region 3 respectively.

CASE-3: When both load and speed change:

Loss model control of 1 hp induction motor drive for a mine hoist load diagram is simulated with MATLAB.

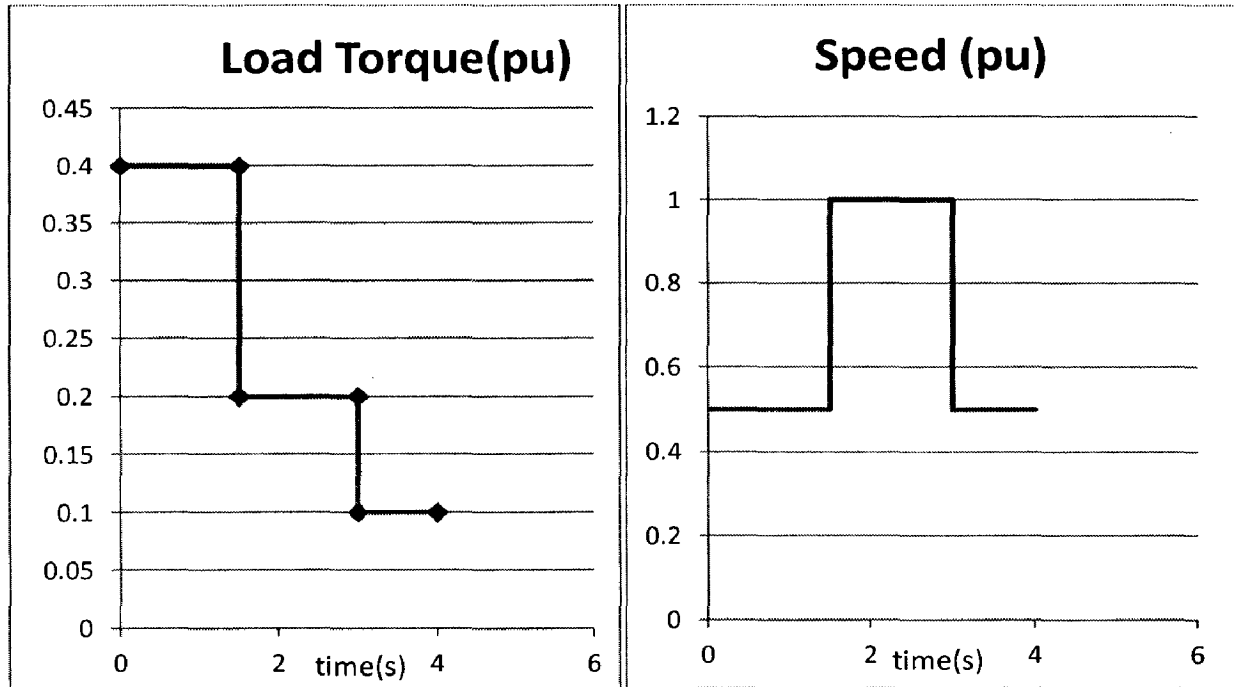


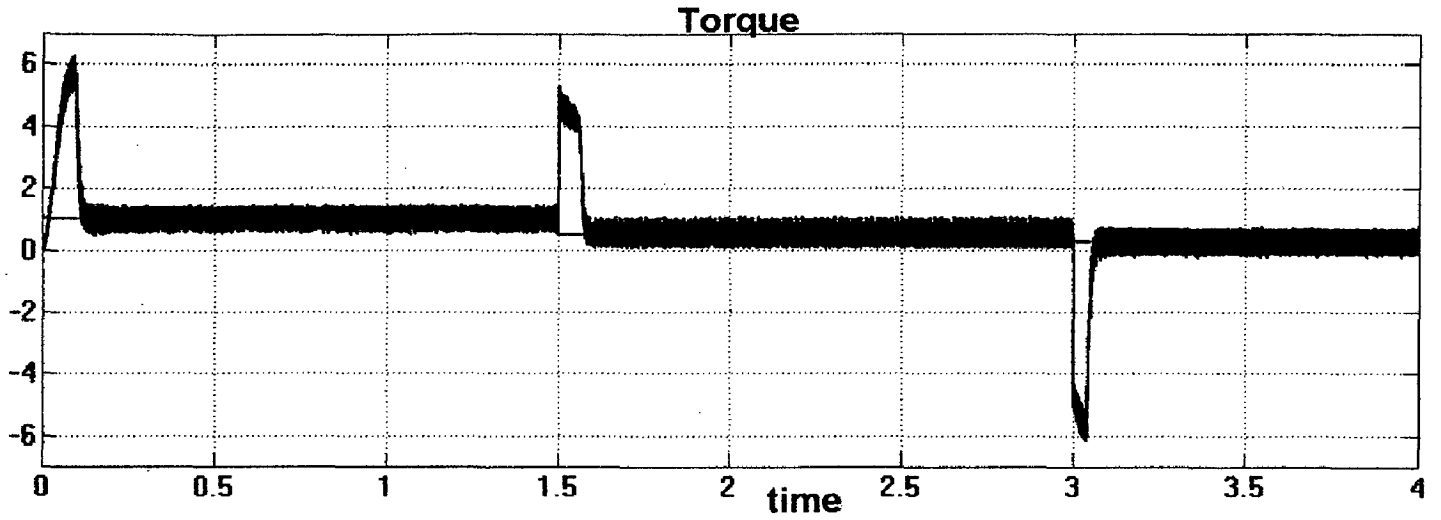
Fig.6.7 Mine hoist load diagram

The load diagram of mine hoist in a mineral industry is shown in Fig.6.7.

Region 1(0-1.5 s): load torque=1 Nm (0.4 pu), Speed=150 rad/s (0.5 pu)

Region 2(1.5-3 s): load torque=0.5 Nm (0.2 pu), Speed=300 rad/s (1 pu)

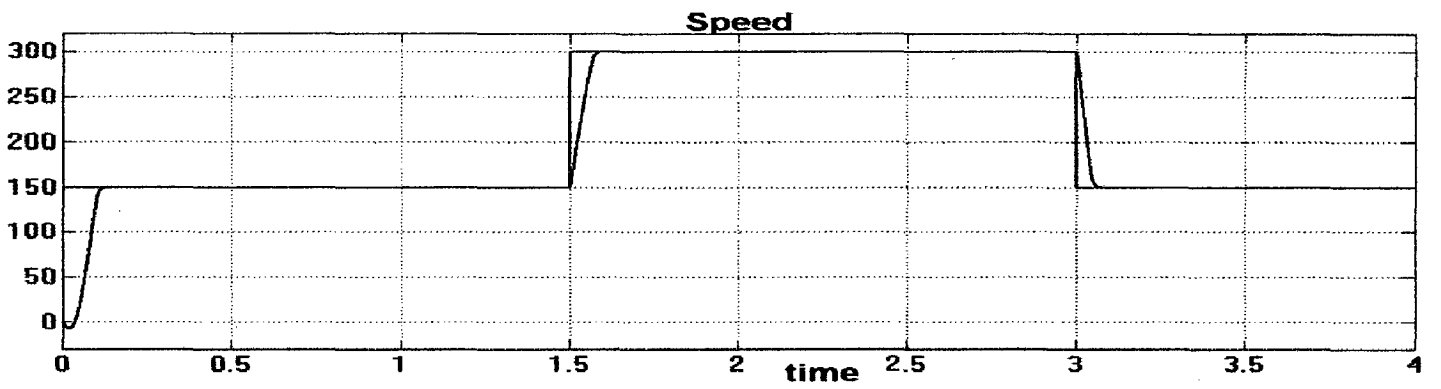
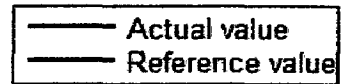
Region 3(3-4 s): load torque=0.25 Nm (0.1 pu), Speed=150 rad/s (0.5 pu)



Region 1:
Torque=1 Nm

Region 2:
Torque= 0.5 Nm

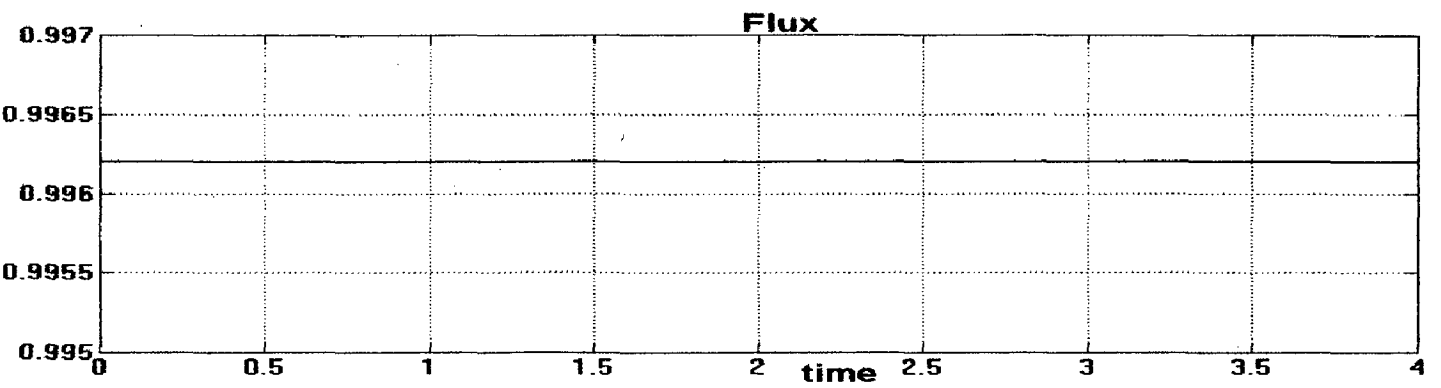
Region 3:
Torque= 0.25 Nm



Region 1:
Speed=150 rad/s

Region 2:
Speed = 300 rad/s

Region 3:
Speed = 150 rad/s



Flux=0.9962 pu.

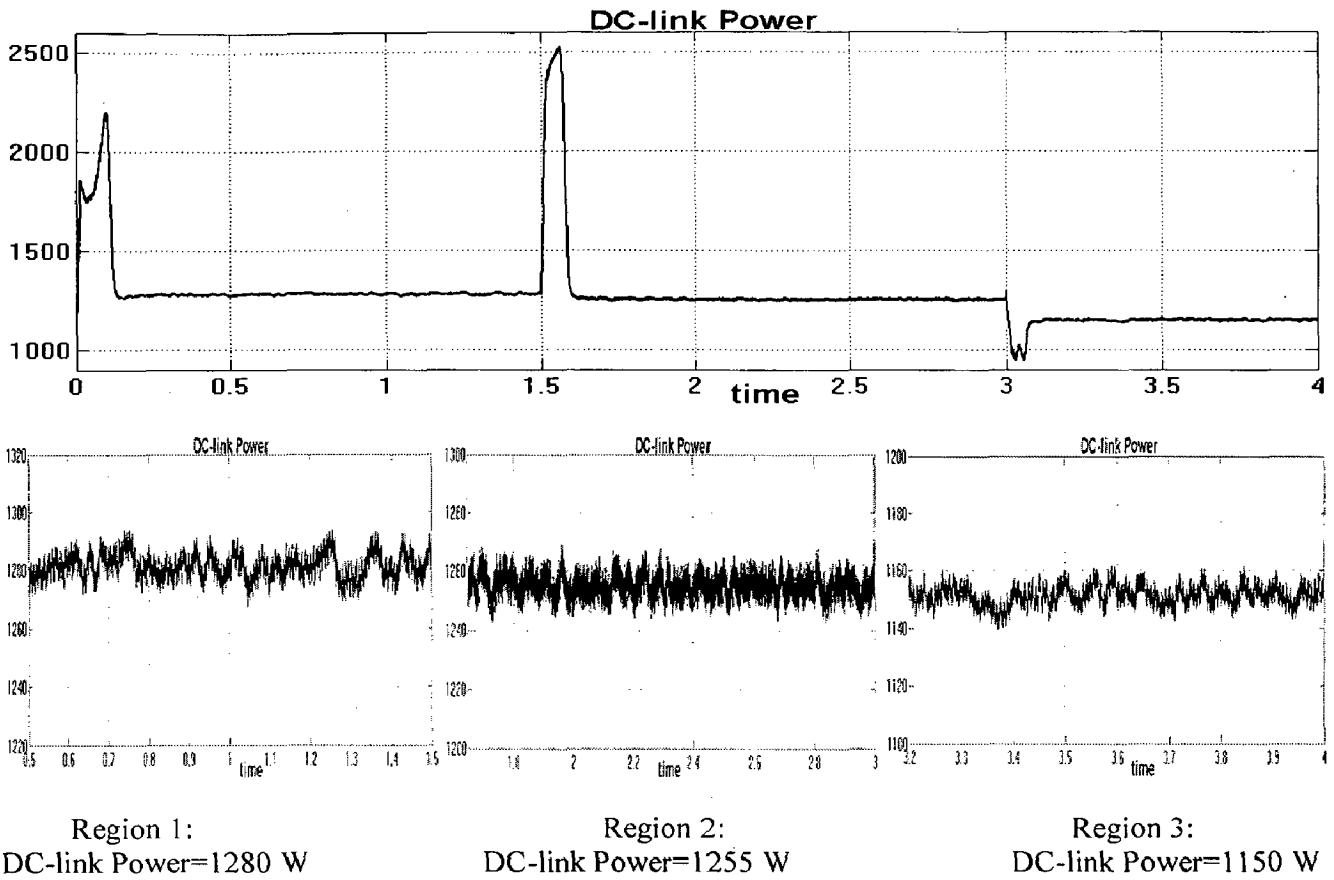
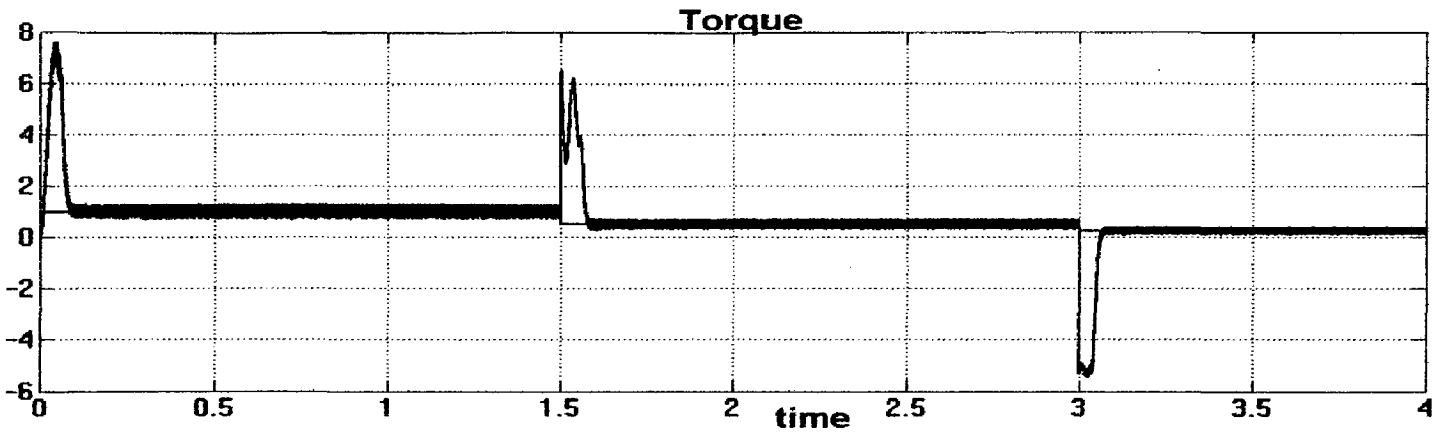


Fig.6.8 Simulation results of vector controlled induction motor drive without loss model control (speed, load change)

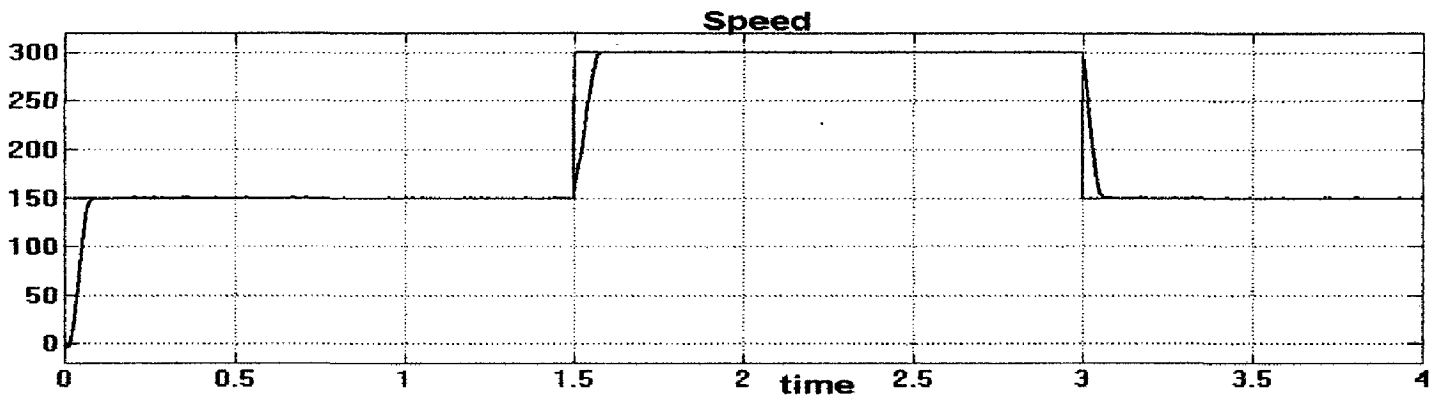
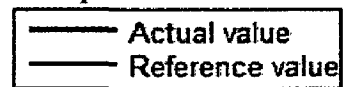
In this case, a mine hoist load diagram is considered where both speed and load torque are varied. Flux is always constant (0.9962 pu) irrespective of variation in speed and torque. Motor consumes DC-link power of 1280 W in region 1, 1255 W in region 2 and 1150 W in region 3.



Torque=1 Nm

Torque= 0.5 Nm

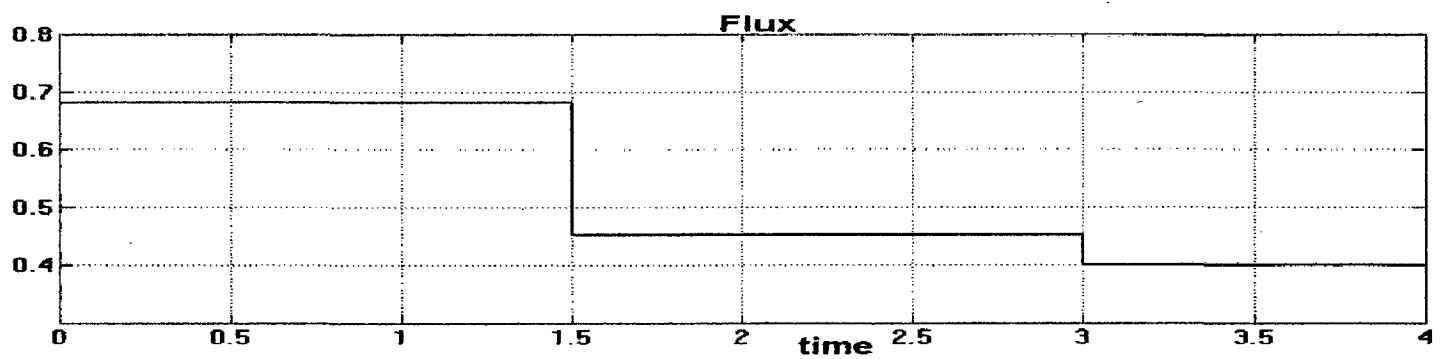
Torque= 0.25 Nm



Region 1:
Speed=150 rad/s

Region 2:
Speed = 300 rad/s

Region 3:
Speed = 150 rad/s



Region 1:
Flux=0.6818 pu

Region 2:
Flux = 0.4532 pu

Region 3:
Flux = 0.4 pu

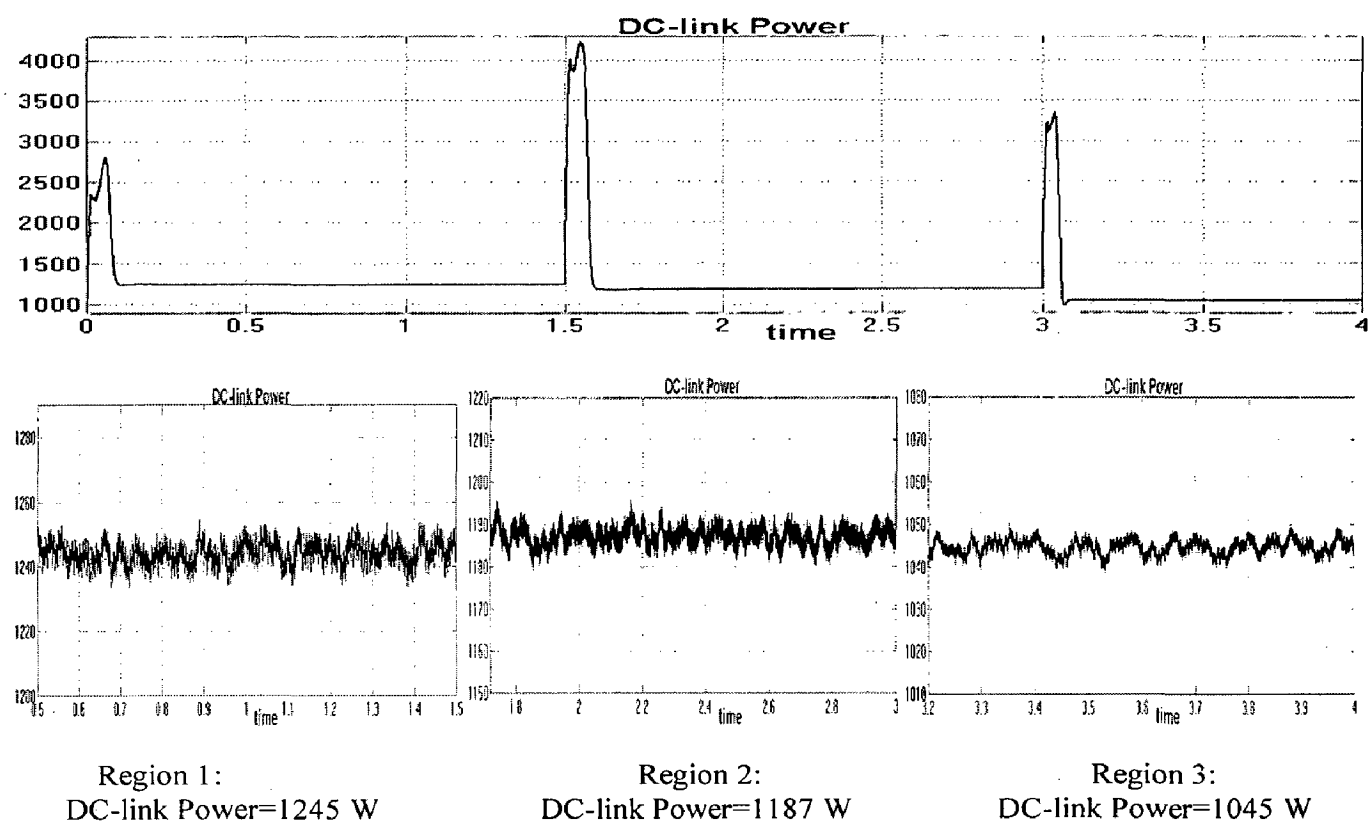


Fig.6.9 Simulation results of energy efficient vector controlled induction motor drive with loss model control (speed, load change)

The two control variables here are load and speed. When LMC is used, flux changes as load and speed are changed. In region 1, load torque is 1 Nm and speed is 150 rad/s. In region 2, both load torque and speed are changed to 0.5 Nm and 300 rad/s respectively. Thus, flux drops from 0.6818 pu to 0.4532 pu. But in region 3, load torque is very low (0.25 Nm) so as speed (150 rad/s). Hence, flux being dependent on these two values drops from 0.4532 pu to 0.4 pu. DC link power to the motor with loss model controller is 35 W lesser (saving) than conventional controller in region 1. Similarly, in region 2, DC link power to the motor with LMC is 68 W lesser than conventional controller. In region 3, DC link power to the motor with LMC is 105 W lesser than conventional controller.

Induction motor parameters vary with temperature. So, parameters obtained by conducting no load and blocked rotor test may vary with loading of induction motor. LMC is sensitive to parameter variation and its performance is affected when parameters change. An attempt is made to gain a deeper physical insight into the induction motor operation through sensitivity analysis of its equivalent circuit parameters. The study reveals the effect each of the circuit parameters namely R_s , R_r , L_s , L_r and L_m has on torque, speed, flux and DC-link power respectively.

The proposed work involves sensitivity analysis of loss model controlled induction motor drive under parameter variation. Simulations are carried out for 420V, 50 Hz, 2 pole, 1 hp motor whose equivalent circuit parameters are

$R_s = 11.124$ ohms, $R_r = 8.9838$ ohms, $L_s = 0.03336$ H, $L_r = 0.03336$ H, $L_m = 0.49045$ H, Moment of inertia = 0.0018 kg-m^2 , Rated torque = 2.5 Nm , Rated speed = 300 rad/s .

Fig.6.11 to Fig.6.16 show simulation results of vector controlled induction motor drive with LMC when each of the motor parameters- R_s , R_r , L_s , L_r and L_m are varied by 20%. Table I and Table II show the effect of various parameters on performance variables-torque, speed, flux and DC-link power when each of the parameters is varied by 20% under loss model control operation and constant flux control operation respectively. Similarly, Table III and Table IV show the effect of parameters on torque, speed, flux and DC-link power when each of the parameters is varied by 10 % under loss model control operation and constant flux control operation respectively.

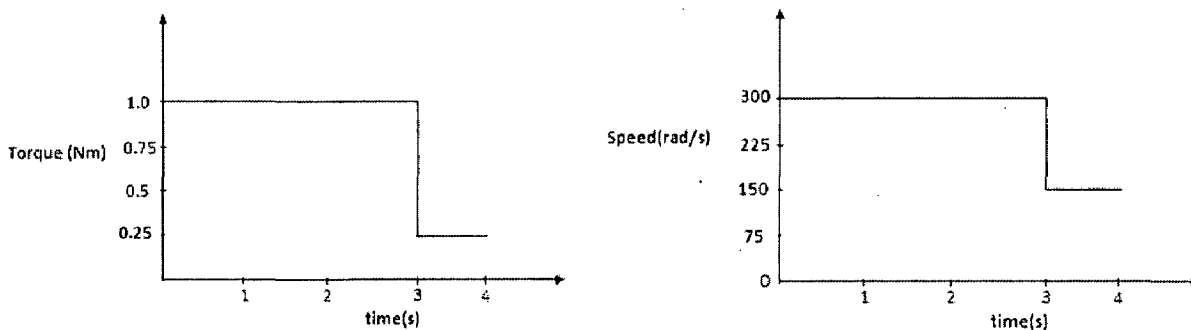


Fig.6.10. Load diagram for sensitivity analysis of LMC under parameter variation

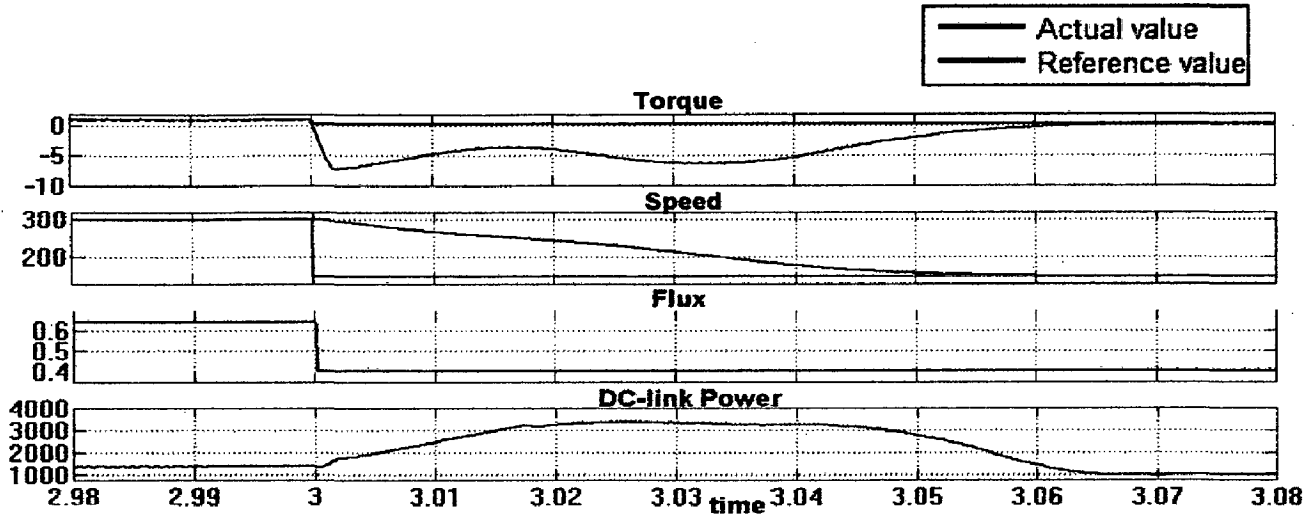


Fig.6.11. Simulation results of vector controlled induction motor drive with LMC under normal operating conditions when none of the parameters is varied ($R_s=11.124$ ohm; $R_r=8.9838$ ohm; $L_s=33.36$ mH; $L_m=490.45$ mH; $L_r=33.36$ mH)

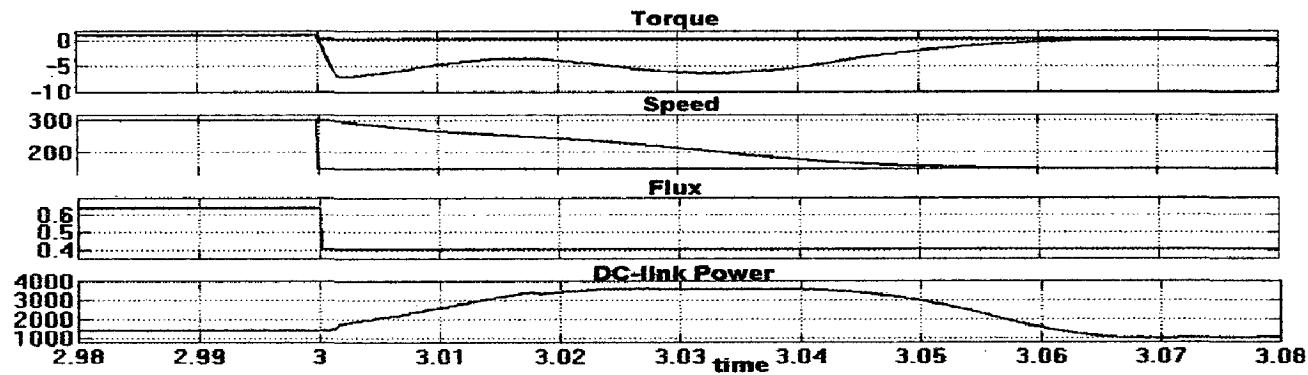


Fig.6.12. Simulation results of vector controlled induction motor drive with LMC when R_s is increased by 20% ($R_s=13.3488$ ohm; $R_r=8.9838$ ohm; $L_s=33.36$ mH; $L_m=490.45$ mH; $L_r=33.36$ mH)

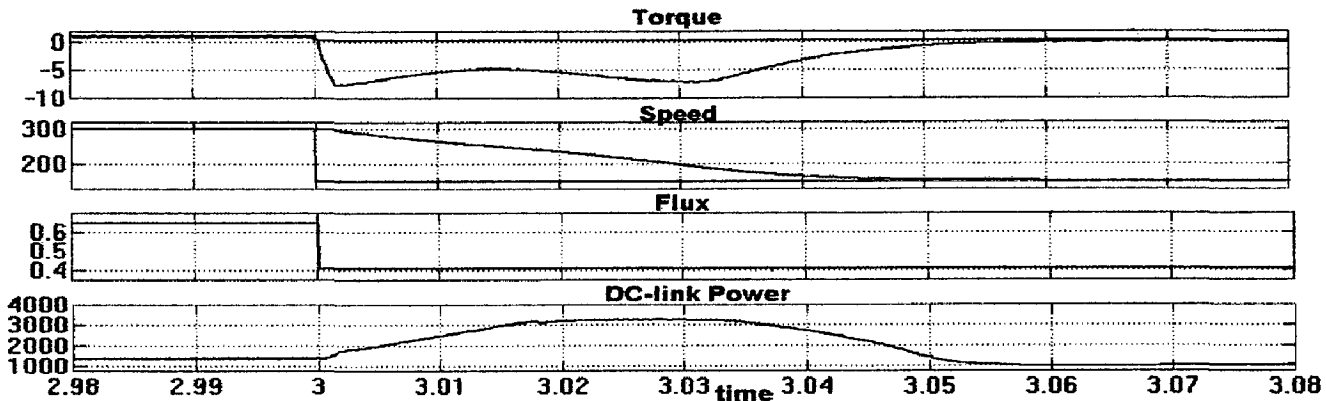


Fig.6.13. Simulation results of vector controlled induction motor drive with LMC when R_r is increased by 20% ($R_s=11.124$ ohm; $R_r=10.78056$ ohm; $L_s=33.36$ mH; $L_m=490.45$ mH; $L_r=33.36$ mH)

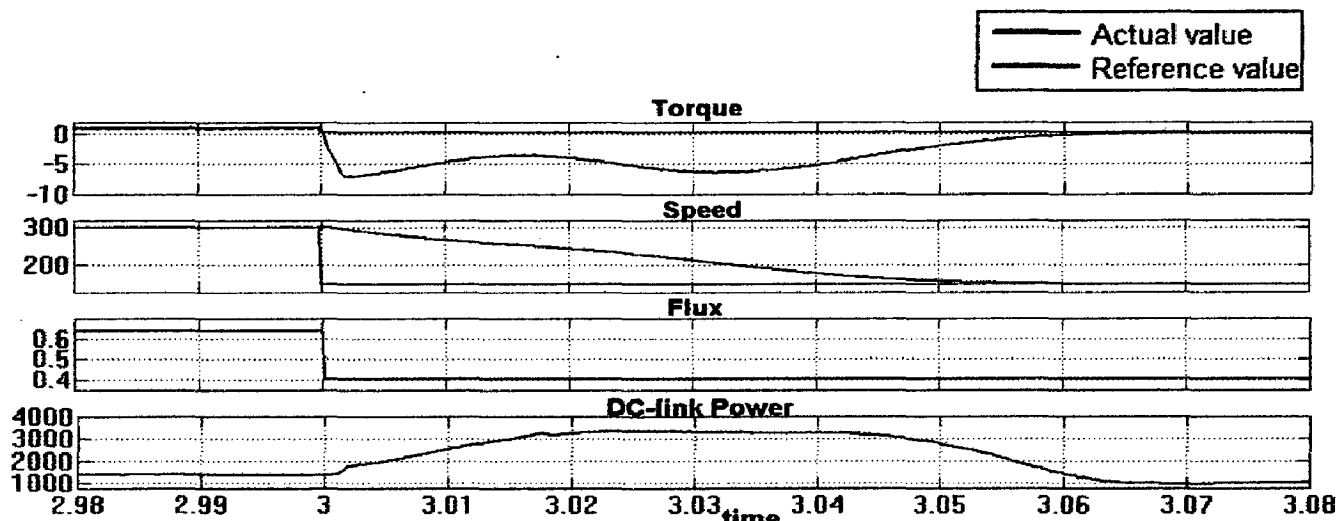


Fig.6.14. Simulation results of vector controlled induction motor drive with LMC when L_s is increased by 20% ($R_s=11.124$ ohm; $R_r=8.9838$ ohm; $L_s=40.032$ mH; $L_m=490.45$ mH; $L_r=33.36$ mH)

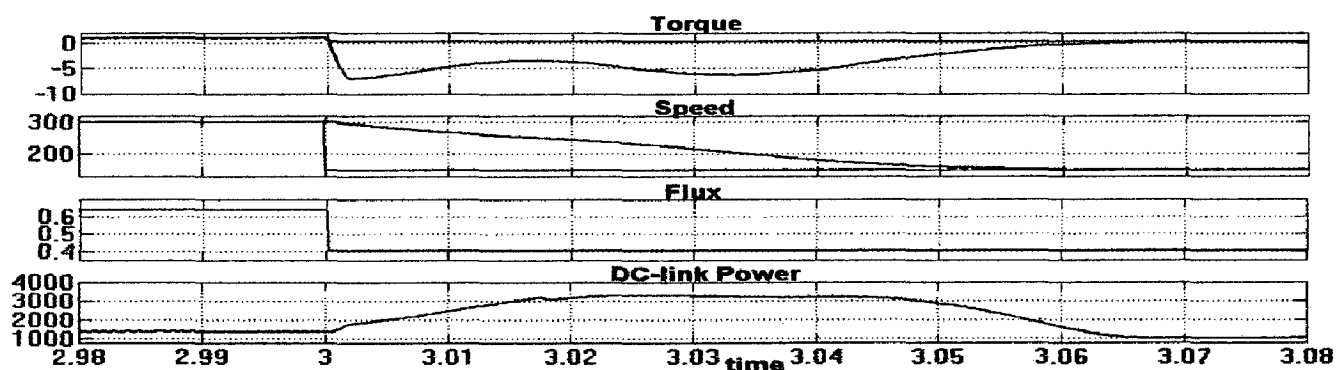


Fig.6.15. Simulation results of vector controlled induction motor drive with LMC when L_r is increased by 20% ($R_s=11.124$ ohm; $R_r=8.9838$ ohm; $L_s=33.36$ mH; $L_m=490.45$ mH; $L_r=33.36$ mH)

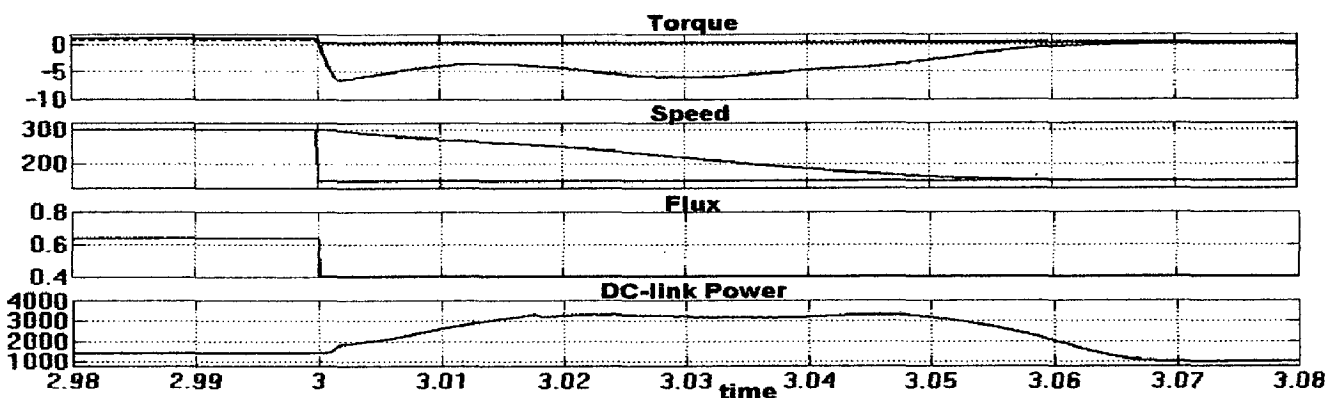


Fig.6.16. Simulation results of vector controlled induction motor drive with LMC when L_m is decreased by 20% ($R_s=11.124$ ohm; $R_r=8.9838$ ohm; $L_s=33.36$ mH; $L_m=392.36$ mH; $L_r=33.36$ mH)

Table 6.2 Motor performance when parameters are changed by 20% under LMC operation

Parameter varied	Torque	Speed	Flux (pu)		DC-link Power (W)	
	Undershoot (Nm)	Settling time(s)	Initial	Final	Over shoot	Final value
Normal condition	-7.3	3.0595	0.637	0.4022	3387	1045
$R_s(+20\%)$	-7.2	3.0589	0.6401	0.4022	3600	1047
$R_r(+20\%)$	-7.8	3.0573	0.6452	0.4087	3244	1047
$L_s(+20\%)$	-7.175	3.0587	0.637	0.4022	3344	1044
$L_r(+20\%)$	-7.14	3.0591	0.639	0.4036	3324	1045
$L_m(-20\%)$	-6.61	3.0605	0.637	0.4022	3317	1052

Table 6.3 Motor performance when parameters are changed by 20% under constant flux operation

Parameter varied	Torque	Speed	Flux (pu)	DC-link Power (W)	
	Undershoot (Nm)	Settling time(s)		Under shoot	Final value
Normal condition	-5.845	3.0523	0.9962	934.72	1150
$R_s(+20\%)$	-5.824	3.0527	0.9962	941	1162
$R_r(+20\%)$	-5.85	3.0521	0.9962	930	1155
$L_s(+20\%)$	-5.9	3.0523	0.9962	937	1155
$L_r(+20\%)$	-5.76	3.0527	0.9962	939	1155
$L_m(-20\%)$	-4.72	3.0611	0.9962	971	1140

Table 6.4 Motor performance when parameters are changed by 10% under LMC operation

Parameter varied	Torque	Speed	Flux (pu)		DC-link Power (W)	
	<i>Undershoot (Nm)</i>	<i>Settling time(s)</i>	<i>Initial</i>	<i>Final</i>	<i>Over shoot</i>	<i>Final value</i>
Normal condition	-7.3	3.0595	0.637	0.4022	3387	1045
R _s (+10%)	-7.235	3.0589	0.6384	0.4031	3467.5	1045
R _r (+10%)	-7.6	3.0581	0.641	0.4058	3316	1046
L _s (+10%)	-7.25	3.0587	0.637	0.4022	3359	1045
L _r (+10%)	-7.15	3.0591	0.6376	0.4036	3336.5	1045
L _m (-10%)	-7.1	3.0591	0.637	0.4022	3336	1048

Table 6.5 Motor performance when parameters are changed by 10% under constant flux operation

Parameter varied	Torque	Speed	Flux (pu)	DC-link Power (W)	
	<i>Undershoot (Nm)</i>	<i>Settling time(s)</i>		<i>Under shoot</i>	<i>Final value</i>
Normal condition	-5.845	3.0523	0.9962	934.72	1150
R _s (+10%)	-5.84	3.0523	0.9962	933.1	1160
R _r (+10%)	-5.87	3.0523	0.9962	933.3	1150
L _s (+10%)	-5.9	3.0523	0.9962	934	1155
L _r (+10%)	-5.82	3.0525	0.9962	933	1155
L _m (-10%)	-5.3	3.0557	0.9962	939.2	1155

Sensitivity analysis of LMC under parameter variation is carried out for 20% and 10% change in motor parameters respectively. The results are compared with constant flux operation where LMC is not used. We notice that the effect of parameter variation is more profound in case of LMC. Torque undershoot is more when LMC is used. This is due to sudden change in flux. Also settling time of speed is more in case of LMC. Since, load and speed are varied, flux being dependent on these two values changes when LMC is used unlike constant flux operation where

flux remains constant irrespective of variation in speed and torque. Overshoot in DC-link power is higher when LMC is used than corresponding undershoot in DC-link power in case of constant flux operation. However, the final steady state value of power under light load condition is lower when LMC is operated. Hence, input DC-link power to the inverter is low and efficiency of the drive system is high. Therefore, optimal energy controller can be used for improving the efficiency of induction motor drive system under partially loaded conditions.

More the variation in parameters more is the overshoot/undershoot in DC-link power under LMC operation and constant flux operation. Also, the final steady state value of power is less when the variation in parameters is less. We also observe that LMC is more sensitive to parameter variation. The performance of LMC controller is based on the accuracy of induction motor parameters. Induction motor parameters vary with temperature. So parameters obtained by conducting no load and blocked rotor test may vary with loading of induction motor. This problem can be solved by using on line estimation. The exact knowledge of some of the induction motor parameters is very important to implement efficient control schemes.

Conclusion

7.1 Conclusion:

The dissertation work is carried in the field of efficiency optimization of induction motor drive through loss model control. The part load operation of induction motors cannot be avoided in many industrial applications like spinning drive in textile industry and hoist drive in mineral industry. The part load efficiency and power factor can be improved by adjusting the magnetizing level in accordance with load and speed. For energy efficient control, flux level in a machine was adjusted by finding optimal value of d axis current to give minimum operating cost or minimum input energy.

Mathematical model of the entire induction motor drive system was presented. Sinusoidal pulse width modulated current controllers were modelled and used in the drive. Optimal energy controller was designed through the loss models of entire variable speed drive system. Motor loss model has been performed with the help of single phase equivalent circuit. Loss model of motor was developed for vector control scheme. Using the PWM inverter, induction motor, speed controller and energy controller the complete drive was simulated with MATLAB/SIMULINK and the performance was evaluated. Loss model based controller has been applied for different variations in speed and load to achieve minimum DC link power under lightly loaded conditions. The superiority of LMC over conventional constant flux control can be seen in terms of reduction in DC-link power under partially loaded conditions. The effect of each of the circuit parameters namely R_s , R_r , L_s , L_r and L_m (for 10% and 20% change) on torque, speed, flux and DC-link power respectively is studied under LMC operation and constant flux operation. It is observed that LMC is more sensitive to parameter variation as compared to constant flux operation. However, the final steady state value of power under light load condition is lower when LMC is operated. Hence, input DC-link power to the inverter is low and efficiency of the drive system is high. Therefore, optimal energy controller can be used for improving the efficiency of induction motor drive system under partially loaded conditions. However, LMC is sensitive to parameter variation.

7.2 Future scope:

The performance of LMC controller is based on the accuracy of induction motor parameters. Induction motor parameters vary with temperature. So parameters obtained by conducting no load and rotor blocked test may vary with loading of induction motor. This problem can be solved by using on line estimation. Also speed and torque overshoot/undershoot are high while using LMC due to sudden change in flux. Advanced techniques involving filter are being developed to minimize this problem. In addition to this, advanced control techniques like ANN, FUZZY and recent developments in PSO in the field of optimization are very useful to find optimal value of flux.

References:

- [1] M.Nasir Uddin and Sang Woo Nam, "New Online Loss-Minimization-Based Control of an Induction Motor Drive," IEEE Transactions on Power Electronics, Vol. 23, no.2, March 2008, pp.926-933.
- [2] J. C. Moreira, T. A. Lipo and V. Blasko, "Simple efficiency maximizer for an adjustable frequency induction motor drive," IEEE Transactions on Industrial Application, Vol. 27, No. 5, Sep./Oct. 1991, pp. 940–946.
- [3] I. Kioskesidis, N. Margaris, "Loss minimization in induction motor adjustable speed drives," IEEE Transactions on Industrial Application, Vol. 43, No. 1, 1996, pp. 226-231.
- [4] Garcia, G.O., Luis, J.C.M., Stephan, R.M., and Watanabe, E.H., "An efficient controller for an adjustable speed induction motor drive," IEEE Transactions on Industrial Electronics, 41, (5),1994, pp. 533–539.
- [5] Lorenz, R.D., and Yang, S.M, "Efficiency-optimized flux trajectories for closed-cycle operation of field-orientation induction machine drives," IEEE Transactions on Industrial Application, 28, (3), 1992, pp. 574–580.
- [6] Sul, S.K., and Park, M.H., "A novel technique for optimal efficiency control of a current-source inverter-fed induction motor," IEEE Transactions on Power Electronics, 3, (2), 1988, pp. 192–199.
- [7] Kirschen, D.S., Novotny, D.W., and Lipo, T.A., "On-line efficiency optimization of a variable frequency induction motor drive," IEEE Transactions on Industrial Application, 21, (4), 1985, pp. 610–615
- [8] Sousa, G.C.D., Bose, B.K., and Cleland, J.G., "A fuzzy logic based on-line efficiency optimization control of an indirect vector-controlled induction motor drive," IEEE Transactions on Industrial Electronics, 42, (2), 1995, pp. 192–198.
- [9] Kim, G.K., Ha, I.J., and Ko, M.S., "Control of induction motors for both high dynamic performance and high power efficiency," IEEE Transactions on Industrial Electronics, 39, (4), 1992, pp. 323–333.
- [10] M.Nasir Uddin and Sang Woo Nam, "Adaptive back stepping based online loss minimisation control of an IM drive," IEEE Transactions on Power Electronics, Vol. 23, No.2, March 2008, pp.926-933.

- [11] C. Chakraborty and Y. Hori, "Fast efficiency optimization techniques for the indirect vector-controlled induction motor drives," *IEEE Transactions on Industrial Application*, Vol. 39, No. 4, Jul./Aug. 2003, pp. 1070–1076.
- [12] S. Lim and K. Nam, "Loss-minimizing control scheme for induction Motors," *IEEE Proceedings-Electronic Power Applications*, Vol. 151, No. 4, July 2004, pp.385-397.
- [13] C. Thanga Raj, S. P. Srivastava and Pramod Agarwal, "Energy Efficient Control of Three-Phase Induction Motor," - A Review, *International Journal of Computer and Electrical Engineering*, Vol. 1, No. 1, April 2009, pp.1793-1898.
- [14] Liu, J., J. Sun, and W. Xu., "Quantum-behaved particle swarm optimization with adaptive mutation operator," *ICNC, Part I, Berlin Heidelberg: Springer-Verlag (2006)*, 959–967.
- [15] Bounekhla, M., Zaim, M. E. and Rezzoug, A., "Comparative study of three minimization methods applied to the induction machine parameters identification using transient stator current," *Electric Power Components and systems*, Vol. 33, 2005, pp. 913-930.
- [16] B. Renier, K. Hameyer, Member and R. Belmans, "Comparison of standards for determining efficiency of three phase induction motors," *IEEE journal*, 1999.
- [17] Nangsue, P., P. Pillay, and S. E. Conry, "Evolutionary algorithms for induction motor parameter determination," *IEEE Transaction on Energy Conversion*, 14 (3), 1999, pp.447–453.
- [18] Benaidja, N., and N. Khenfer, "Identification of asynchronous machine parameters by evolutionary techniques," *Electric Power Components and Systems*, 34, 2006, pp.1359–1376.
- [19] Ursem, R. K., and P. Vadstrup, "Parameter identification of induction motors using differential evolution," In *Proc. IEEE congress on Evolutionary Computation*, New Jersey, USA, IEEE Press 2003, pp.790–796.
- [20] Ursem, R. K., and P. Vadstrup, "Parameter identification of induction motors using stochastic optimization algorithms," *Applied Soft Computing* 4 (1), 2004, pp.49–64.
- [21] Auinger H., "Determination and designation of the efficiency of electrical machines," *Power engineering journal* (1999).

- [22] A. Boglietti, A. Cavagnino, M. Lazzari, M. Pastorelli., "Induction Motor Efficiency Measurements in accordance to IEEE 112-B, IEC 34-2 and JEC-37 International Standards," IEEE journal (2003).
- [23] Kennedy, J. and Eberhart, R., "Particle Swarm Optimization," IEEE International Conference on Neural Networks (Perth, Australia), IEEE Service Center, Piscataway, NJ, 1995, pp. IV: 1942-1948.
- [24] R.Thangaraj, C. Thanga Raj, Millie Pant, Attulya K. Nagar., "In-Situ Efficiency Determination of Induction Motor: A Comparative Study of Evolutionary Techniques," Application of Artificial Intelligence, Vol. 25, No. 2, 2011, pp.116-140.
- [25] Pillay, P., V. Levin, P. Otaduy, and J. Kueck., "In situ induction motor efficiency determination using genetic algorithm," IEEE Transaction on Energy Conversion, 13 (4), 1998, pp.326-333.

List of Publications:

1. Anil Chandrakanth.S, Thanga Raj Chelliah, S.P.Srivastava, Radha Thanga Raj, "In-situ efficiency determination of induction motor through parameter estimation," in Proc. International Conference on soft computing for problem solving (SocPros-2011)- Springer, Roorkee, Vol.1, Dec 20-22, 2011, pp.655-666. (Paper published) <http://www.springerlink.com/content/91p8281284642860/>
2. Anil Chandrakanth.S, S.P.Srivastava, "Sensitivity analysis of loss model controller under parameter variation," in Proc.International Conference on Advances in Electronics, Electrical and Computer Science Engineering-EEC 2012. (Paper Accepted)
3. Anil Chandrakanth.S, S.P.Srivastava, Thanga Raj Chelliah, "Sensitivity analysis of loss model controller under parameter variation," in Proc. IEEE INDICON-2012. (Paper under review)
4. Anil Chandrakanth.S, Thanga Raj Chelliah, S.P.Srivastava, Radha Thanga Raj, "Efficiency determination of induction motor using particle swarm optimization," International Journal of Advanced Intelligence Paradigms (IJAIP) (SocPros-2011). (Reply is awaited)

Appendix-A:

A.1 MATLAB/SIMULINK Model for Loss Model Control of Induction Motor:

The complete MATLAB, SIMULINK model of loss model control is shown in Fig.A.1. This model mainly consists of speed controller, loss model controller, flux angle calculation, vector control and current controller which are later integrated individually as shown in Fig.A.2 - A.7.

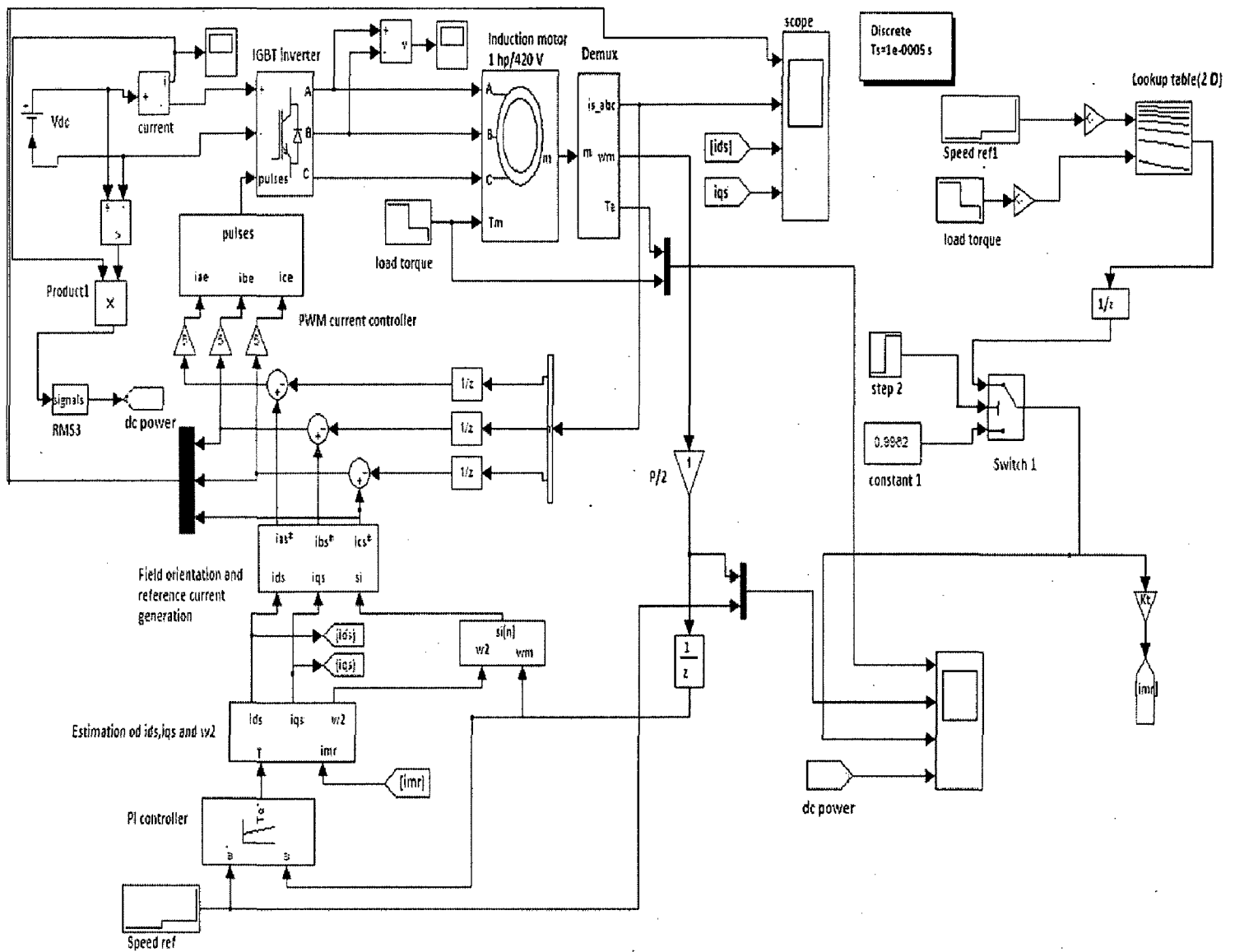


Fig.A.1 MATLAB/SIMULINK model of loss model control of induction motor

A.1.1 PI speed controller:

The MATLAB/SIMULINK model of the PI controller in discrete time is shown in Fig.A.2. The reference torque is calculated using the proportional and integral gain parameters, k_p and k_i respectively along with the limiter.

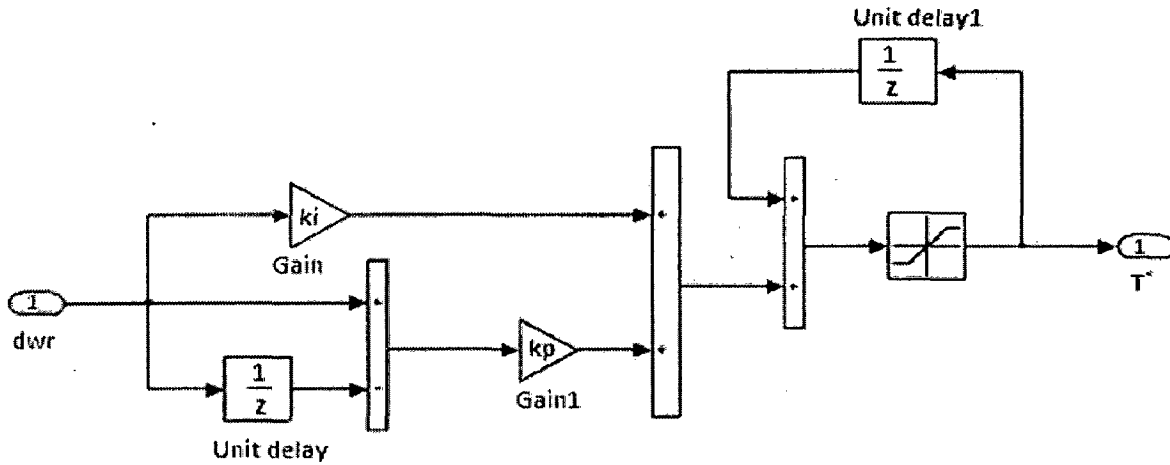


Fig.A.2 Discrete PI controller in MATLAB

This model is developed based on following equations.

$$m(t) = k_p e(t) + k_i \int_0^t e(t) dt \quad \text{A.1}$$

Discrete zing the above equation,

$$M(z) = K_p E(z) + K_i E(z)/(1-z^{-1})$$

$$M(z) (1-z^{-1}) = (K_p (1-z^{-1}) + k_i) E(z)$$

$$M(z) = (K_p (1-z^{-1}) + k_i) E(z) + M(z) z^{-1} \quad \text{A.2}$$

A.1.2 Vector controller:

This section calculates the direct and the quadrature axis stator current components i.e. i_{ds}^* and i_{qs}^* . Mathematical equations are given as

$$i_{ds}^* = i_m + \tau_r \frac{di_m}{dt} \quad \text{A.3}$$

$$i_{qs}^* = \frac{T^*}{k i_{mr}^*} \quad \text{A.4}$$

$$\omega_2^* = \frac{i_{qs}^*}{\tau_r i_{mr}^*} \quad \text{A.5}$$

$$k = \frac{3}{2} \frac{P}{2} \frac{M}{1 + \sigma_r} \quad \text{A.6}$$

Where, $\tau_r = \frac{L_r}{R_r}$ is the rotor time constant.

P is the number of poles, M is the mutual inductance, i_{ds}^* and i_{qs}^* refer to flux and torque components of stator current, σ_r is the rotor leakage factor, R_r and L_r are the rotor resistance and rotor self inductance respectively.

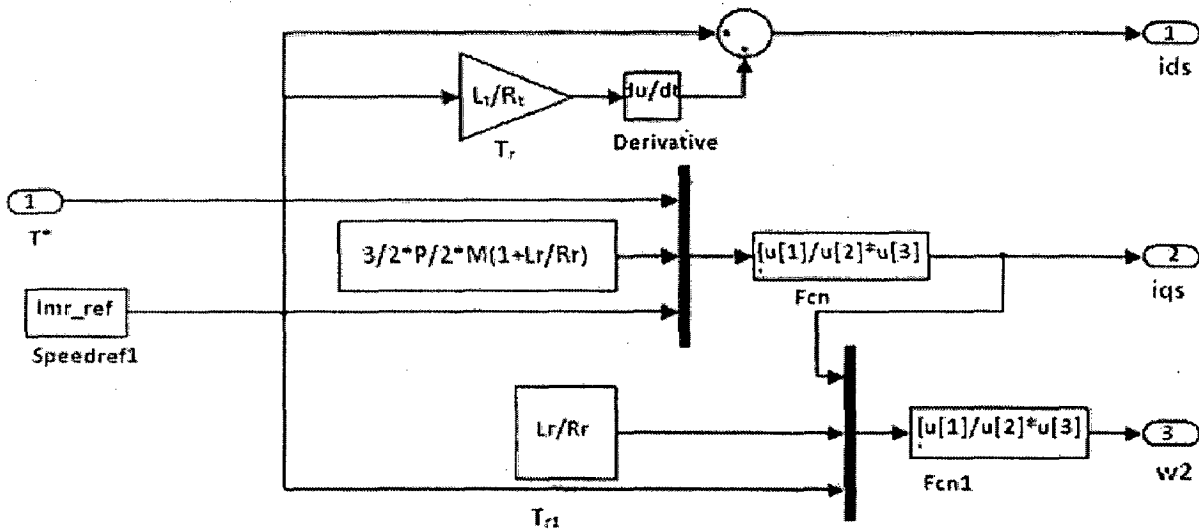


Fig.A.3 Vector controller

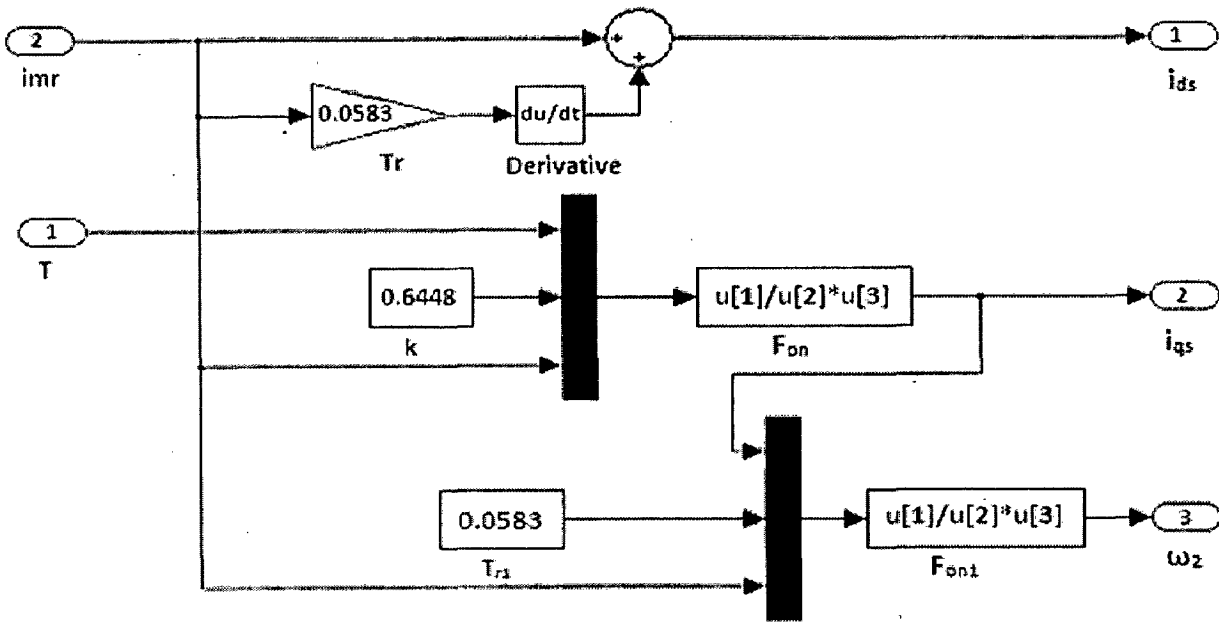


Fig.A.4 MATLAB model for the estimation of i_{ds}^* , i_{qs}^* and ω_2^* .

A.1.3 Three phase reference current generation:

Once the flux angle and d-q components of the reference currents are calculated, the required three phase currents are calculated in the stationary reference frame. The required transformation for dq components to abc components is given as below,

$$i_{as}^* = -i_{qs}^* \sin \varphi + i_{ds}^* \cos \varphi \quad \text{A.8}$$

$$i_{bs}^* = 0.5 * i_{ds}^* (-\cos \varphi + \sqrt{3} \sin \varphi) + 0.5 * i_{qs}^* (\sin \varphi + \sqrt{3} \cos \varphi) \quad \text{A.9}$$

$$i_{cs}^* = -(i_{as}^* + i_{bs}^*) \quad \text{A.10}$$

Where i_{as}^* , i_{bs}^* and i_{cs}^* are three phase currents in stator reference frame and i_{ds}^* , i_{qs}^* refer to decoupled components of stator current i_s^* in two phase system.

The MATLAB models for calculating flux angle in discrete frame with sample time of $10e-6$ is shown in Fig.A.5 and MATLAB model for finding out three phase reference currents is shown in Fig.A.6.

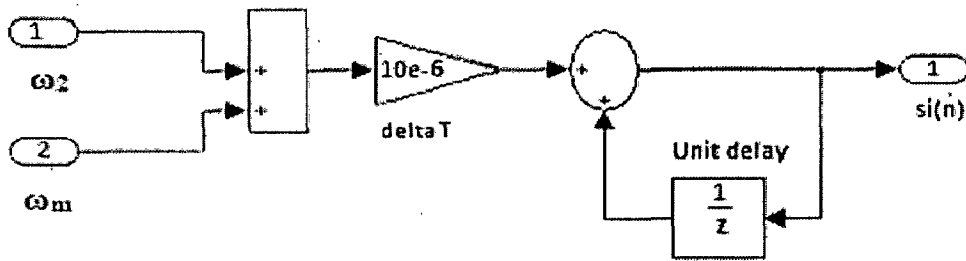


Fig.A.5 MATLAB model for calculating flux angle

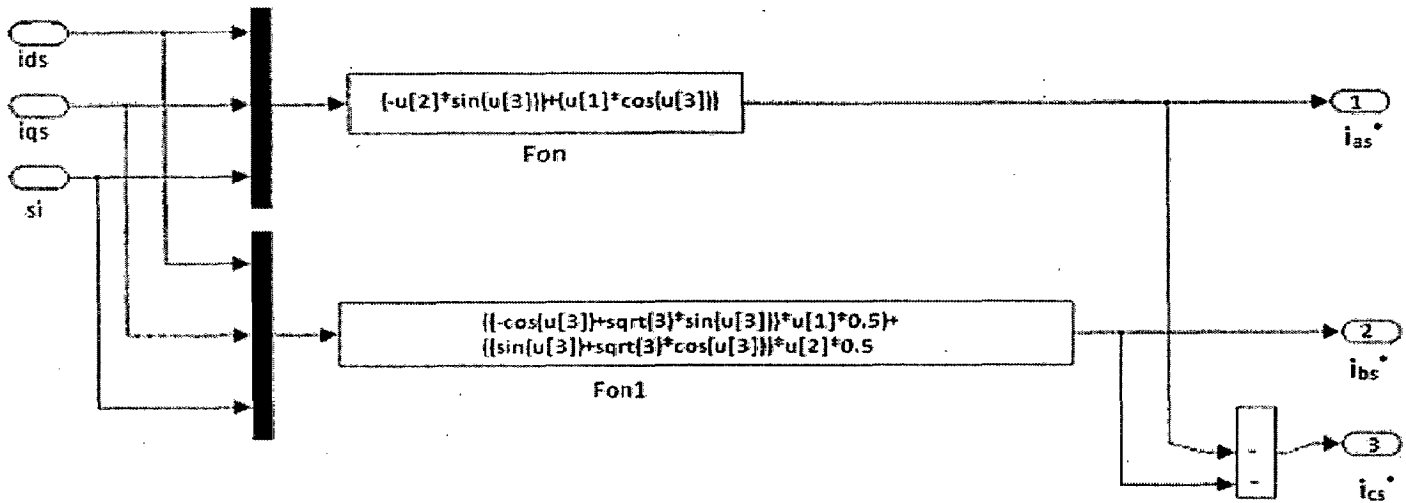


Fig.A.6 MATLAB model for finding out three phase reference currents

A.1.4 PWM current controller:

The current error for a phase is defined as the difference between reference current and sensed winding current of that phase. Thus, the current errors in the three phases at kth instant are defined by the following equations.

$$i_{aes}^*(k) = i_{as}^*(k) - i_{as}(k) \tag{A.11}$$

$$i_{bes}^*(k) = i_{bs}^*(k) - i_{bs}(k) \tag{A.12}$$

$$i_{ces}^*(k) = i_{cs}^*(k) - i_{cs}(k) \tag{A.13}$$

The errors obtained as above are given to a proportional controller to generate a modulating signal for each phase. The modulating signal is then compared with a triangular carrier wave to generate a switching signal.